ORIGINAL RESEARCH Open access

A Neural Network-Enhanced Multi-Objective Optimization Framework for Sustainable Energy Management

Luca Ferraro[1*], Matteo Ricci[1], Giulia Moretti[2]

Abstract

This paper presented a gene modification optimization technique reinforced by neural networks, aimed at multi-objective energy resource management. In response to the imperative for sustainable energy strategies, the approach adopted neural network architectures as fitness evaluators, signaling a step forward in AI-powered optimization. Information sourced from the European Union spanned greenhouse gas emissions, source-specific energy consumption, energy imports, and the levelized cost of energy. Because distinct energy consumption source configurations produce differing outcomes in greenhouse gas emissions, expenditure, and import levels, neural network forecasting models were deployed to anticipate how novel energy mixes would affect these indicators. The resulting predictions were then fed into the gene modification optimization workflow to identify superior configurations. Through 28 generations, the simulations indicated a 46% drop in energy costs alongside a 9% decline in emissions. Automating the parameter selection process mitigated the influence of human bias and subjectivity, thus reinforcing the neutrality of the outcomes. Comparisons with established methods, among them Euclidean Distance, corroborated the enhanced effectiveness of the proposed technique. Furthermore, the ability to depict chromosomes and their gene values provided interpretability throughout the optimization process. These findings imply notable progress for the energy field and point to prospective applications in other industries, thereby aiding the worldwide push against climate change.

Keywords Machine learning, Energy management, Multi-objective optimization, Gene modification optimization technique, Greenhouse gas emissions

*Correspondence:
Luca Ferraro
luca.ferraro@unibo.it
[1] Department of Smart Energy Systems Engineering, Faculty of Engineering, University of Bologna, Bologna, Italy
[2] Department of Artificial Intelligence for Electrical Networks, Faculty of Engineering, Polytechnic University of Turin, Turin, Italy

Introduction

As alarm over climate disruption, environmental pollution, and dwindling fossil fuel stocks escalates, the pursuit of ideal energy source stewardship has come to the fore in recent times. The Intergovernmental Panel on Climate Change (IPCC) stresses the pressing requirement to cap planetary warming at 1.5 °C, a goal that demands a prompt pivot away from fossil-based sources toward renewables [1]. A central predicament in the modern global energy arena is refining the energy consumption mix to secure the smallest possible greenhouse gas (GHG) emissions, curb import dependency, and bring down operational outlays, all while accommodating the world's mounting appetite for energy [2].

Coal, oil, and natural gas have traditionally constituted the pillars of global energy architectures owing to their concentrated energy content and ready availability [3]. The entrenched infrastructure and favorable economics surrounding these sources have further cemented their dominance within international energy markets [4]. Nevertheless,

This is an open access article distributed under the terms of the Creative Commons Attribution-NonCommercial-ShareAlike 4.0 International License (CC BY-NC-SA 4.0), which permits non-commercial use, distribution, reproduction, and adaptation in any medium or format, provided that appropriate credit is given to the original author(s) and source, a link to the license is provided, and any changes made are indicated. Adapted material must be distributed under the same license.

© 2023 The Author(s). | Published by Institute of Smart Energy Systems Press

burning them discharges copious volumes of carbon dioxide and other contaminants into the atmosphere, leading to elevated greenhouse gas emissions (GHG) [5]. Beyond that, the exhaustible nature of fossil fuel deposits amplifies anxieties about energy reliability and geopolitical friction [6]. Nuclear power, although an option characterized by comparatively modest GHG releases during generation, is by no means trouble-free, facing obstacles such as the secure handling of radioactive remnants and lasting public disquiet [7]. The relative strengths and weaknesses of nuclear energy remain a fiercely contested subject in specialist forums [8]. By contrast, renewable sources—solar, wind, hydropower, and bioenergy—are beginning to command greater notice because of their capacity to curb GHG emissions and attenuate ecological damage [9]. Still, the fitful nature of renewable generation constitutes a formidable hurdle to its pervasive embedding within current energy systems [10].

Tuning energy source utilization poses several difficulties when viewed through economic, ecological, and societal lenses. Mathematically, one of the foremost hurdles is the nonlinear and non-convex makeup of the underlying problems. Specifically, the interlinkages tying together diverse energy sources, storage mechanisms, demand rhythms, and environmental restrictions are nonlinear, making the identification of a single global optimum a formidable task [11]. What is more, the problem unfolds across a multi-dimensional decision landscape [12]; i.e., settling on the best portfolio of energy sources, their respective capacities, and their dispatch protocols calls for weighing manifold economic considerations, which renders the optimization process computationally onerous [13]. As a consequence, the call for efficient computational procedures and algorithms has turned critical for reaching actionable answers [14], not least because such choices compel policymakers to strike trade-offs shaped by their particular regional circumstances [15].

The European Union (EU) represents an exemplary testbed for examining energy utilization. Its resolute environmental stance, heterogeneous energy amalgamation, economic momentum, and mature regulatory apparatus supply a strong underpinning for the present work [16]. The coexistence of renewables, fossil sources, and nuclear generation across this region enables a sweeping evaluation of the emissions and costs linked to various energy pathways, simultaneously constituting a stringent trial for the GMOT [17].

Recently, the refinement of energy source utilization has been the subject of considerable investigation [18]. Still, a widespread deficiency in extant models lies in the encroachment of human subjectivity when juggling opposing objectives. Put in technical terms, multi-objective optimization seeks to extract a set of Pareto-optimal compromises that faithfully reflect the tensions among clashing goals [19]. Yet the procedure can be unwittingly colored by human preconceptions. For example, scalarization approaches may demand subjective preferential weighting of different goals, possibly warping the Pareto frontier toward certain aims [20]. Evolutionary algorithms, pervasively employed in multi-objective optimization, embed selection operators and settings (e.g., mutation probabilities) that, unless fixed with objective discipline, can direct the exploration toward specific tracts of the solution space [21]. Furthermore, a great many models are encumbered by an excess of hyperparameters, a situation that often begets convoluted tuning and the danger of overfitting [22]. An additional complication is that most optimization frameworks incorporate inherent uncertainties and approximation errors, particularly when constraint observance must be ensured [23].

To remedy these shortcomings, the present study proposes a Neural Network-Enhanced Gene Modification Optimization Technique (GMOT) that harnesses Artificial Neural Networks (ANN) as objective functions. In doing so, GMOT reduces the role of human prejudice in weighing conflicting aims, streamlines the entire procedure, and fosters more impartial decision-making for problems with many dimensions. On top of that, GMOT slashes the quantity of hyperparameters, thereby sidestepping the pitfalls that frequently attend overparameterization. To put it concisely, GMOT ensures that constraints are rigorously satisfied, sweeping away the indeterminacies and approximation inaccuracies that marred antecedent techniques. This marriage of state-of-the-art AI instruments with the logic of genetic optimization spotlights the revolutionary capacity of AI when confronting present-day multi-faceted dilemmas. In sum, this article distinguishes itself through its pioneering method of optimizing energy across the EU, delivering a technique that fuses precision, process efficiency, and impartiality.

© 2023 The Author(s). | Published by Institute of Smart Energy Systems Press

Background

Multi-objective optimization falls under the umbrella of vector optimization, where decision-makers must reconcile two or more competing goals. To meet such challenges, scholars have advanced a range of strategies; a frequently adopted route is the use of metaheuristic algorithms—including genetic algorithms, particle swarm optimization, and simulated annealing—that can traverse the solution space and pinpoint a set of Pareto-optimal alternatives [24]. Another pathway is the application of mathematical programming formalisms such as goal programming or fuzzy programming, which accommodate the framing and resolution of multi-objective optimization tasks involving vague or uncertain inputs [25]. In recent years, growing interest has focused on the blending of machine learning with optimization algorithms to handle multi-objective optimization problems. Machine learning tools, such as neural networks and support vector machines, can be used to construct surrogate models that emulate the behavior of complex energy configurations. Those surrogate models can then be exploited within optimization procedures to accelerate the search trajectory and improve computational throughput [26].

Whichever direction is taken, settling on a fitting cost or fitness function constitutes a fundamental obstacle for any multi-objective optimization methodology, particularly within high-dimensional contexts; one candidate is the global criterion method, which collapses a multi-objective formulation into a single-objective one by shrinking the gap between several reference points and feasible destination regions, with the reference point denoting an ideal configuration [27]. Another candidate is the weighted-sum method [28]; it consolidates every objective into a single measure through a weighting vector, where the weights are customarily normalized [29]. This approach, however, carries two innate shortcomings: the challenge of assigning weights when objectives differ in scale, and a predisposition toward bias when uncovering compromise solutions. Beyond that, it may lose efficacy should the multi-objective problem be non-convex. To sidestep this hurdle, the ε-constraint method can be employed [24]; in this setup, one objective is maximized or minimized while the remaining ones are reformulated as constraints [30]. By altering the ε vector, numerous optimal answers can be harvested. Nevertheless, for certain ε vectors, a feasible solution may not exist [24].

Additionally, the deployment of metaheuristic algorithms, for instance genetic algorithms and particle swarm optimization, has demonstrated effectiveness in addressing complex multi-objective optimization problems. For instance, using such algorithms to refine energy use and reduce greenhouse gas emissions has been examined extensively, revealing considerable performance improvements and long-term viability [31]. That being said, these algorithms often require intensive parameter calibration and can be sensitive to initial conditions, factors that may diminish their robustness and appropriateness in particular scenarios.

Likewise, hybrid optimization approaches that fuse multiple techniques have shown potential to strengthen the resilience and breadth of multi-objective optimization models [32]. The union of fuzzy programming and goal programming with established optimization practices, as a case in point, facilitates a more capable handling of uncertainties and imprecise information, culminating in solutions that are both more trustworthy and more workable [33]. For all their benefits, such hybrid schemes can be demanding to roll out and may require niche expertise to ensure seamless integration and operation.

Moreover, multi-objective optimization paradigms have been applied extensively to hone energy utilization in a variety of systems. For example, a framework built around the Improved Shuffled Frog Leaping Algorithm (ISFLA) was suggested to fine-tune microgrid energy consumption by incorporating Distributed Energy Resources (DERs) [34]. Although ISFLA represents an inventive optimization pathway, it continues to exhibit certain flaws that demand additional refinement, including parameter configuration.

A setup merging Building Information Modeling (BIM), machine learning, and the non-dominated sorting genetic algorithm-II (NSGA II) was proposed to reduce energy usage and improve thermal comfort simultaneously [35]. The proposed methodology is constrained when confronting convoluted and strongly nonlinear optimization settings, given that it leans on particular assumptions and models that may fail to capture every subtlety of the problem landscape.

© 2023 The Author(s). | Published by Institute of Smart Energy Systems Press

A Consumption-based Multi-objective Optimization Model (CMOM) was advanced to curtail energy consumption while upholding economic expansion, drawing on China as an illustrative case [36]. The proposed CMOM framework may encounter difficulties in achieving its aims. Its behavior can be shaped by parameter settings, population size and problem complexity. Another path pursued in multi-objective optimization inside the energy domain entails the fusion of cutting-edge machine learning methods with conventional optimization routines. For example, coupling neural networks with optimization algorithms was used to improve the performance of hybrid photovoltaic and fuel cell installations for the production of green hydrogen and electricity [37].

In view of the approaches enumerated above, the multi-objective optimization of energy resource consumption is beset by several sizable obstacles that warrant deeper investigation and refinement to boost the effectiveness and practical reach of these techniques.

One formidable obstacle is the human influence in setting model hyperparameters, formulating assumptions, and making trade-off calls, all of which can tint the impartiality of the final optimal answer. Hyperparameter tuning is often undertaken manually or with minimal mechanization, letting human prejudice seep into the optimization sequence [38]. This can breed suboptimal answers that fall short of representing the genuine best attainable results. Beyond that, the assumptions woven into the model-building stage can materially color the outputs [39]. These assumptions routinely simplify involved real-world circumstances to make the problem more tractable. Yet, they might concurrently disregard critical elements, leading to solutions that are less precise or less transferable. Trade-off resolutions, which are integral to multi-objective optimization, further intensify this complication, since they demand subjective judgments about the relative weight of distinct objectives [40]. Studies have indicated that incorporating more mechanized and dispassionate methods for setting these parameters can reduce bias and strengthen the robustness of the optimization results [41].

Another obstacle stems from the restrictions inherent in optimization problems. These restrictions must be satisfied with precision to ensure the feasibility and reliability of the solutions while avoiding indeterminacies and approximation errors [42]. In the framework of energy management, restrictions may encompass physical bounds of energy systems, statutory obligations, and sustainability ambitions. It is paramount that these restrictions be truthfully depicted and honored within the optimization constructs. Yet, many prevalent methods struggle to enforce rigorous restriction observance, especially in complex and dynamic environments. This can lead to answers that are optimal in principle but impractical or substandard when applied to real-world contexts [43].

A further difficulty arises from the practice of normalization and vectorization. Although these instruments help reduce the complexity of optimization tasks, they can dilute particularity and objectivity in the examination [44]. These maneuvers recast the original problem into a more wieldy shape, but this reshaping can veil salient details and nuances of the issue under study. As an illustration, normalization can spark interpretability difficulties, since the recast problem might cease to echo the original magnitude and setting of the data [45]. This can impede decision-makers from grasping and placing faith in the optimization outputs, potentially slowing the real-world acceptance of these methods. In a similar vein, vectorization can on occasion bring about an oversimplified picture in which the recast problem sheds essential interdependencies and relationships that were present in the original data. Confronting these obstacles demands the formulation of advanced techniques that can safeguard the specificity and context of the initial problem while continuing to harvest the computational gains conferred by normalization and vectorization.

On top of that, within the field of energy system optimization, a significant difficulty lies in navigating the enormous and convoluted search space of plausible energy source configurations. Established optimization approaches frequently depend on pre-specified and narrow fitness functions. Such approaches customarily work on raw data or pre-set mathematical relationships, a practice that can be constraining and overlook the delicate, nonlinear interdependencies that characterize energy systems. As a consequence, they may steer toward suboptimal outcomes when grappling with the high dimensionality and complex interdependencies typical of real-life circumstances.

© 2023 The Author(s). | Published by Institute of Smart Energy Systems Press

In the present contribution, a Neural Network-Enhanced Gene Modification Optimization Technique tailored to multi-objective energy resource management has been engineered to refine energy consumption sources across the EU. This unprecedented methodology concurrently curtails costs, energy imports, and GHG emissions. At the same time, it ensures demand is strictly met and addresses the hurdles of hyperparameter calibration, constraint compliance, and preserving specificity. By incorporating neural networks as fitness models, the proposed technique improves efficiency and robustness, tangibly reducing human partiality and raising the standard of constraint handling. Moreover, the prospective scope of this method extends well beyond the energy sector into a range of optimization contexts, spanning manufacturing, logistics, and healthcare, thereby attesting to its adaptability and broad relevance. The novelty of GMOT springs from its singular amalgamation of gene modification, neural networks, and evolutionary optimization, a blend that directly confronts the fundamental challenges inherent in multi-objective optimization management.

Materials and Methods

To accomplish the goals of this investigation, the sequence of steps depicted in **Figure 1** was carried out. The procedure began with data compilation. After that, two separate Artificial Neural Networks (ANN) models were constructed and trained to estimate GHG emissions and energy imports. As a concluding phase, a gene modification optimization framework was conceived and executed to improve the allocation of energy sources, so that energy demand would be met while simultaneously achieving reductions in GHG emissions, the Levelized cost of energy (LCOE), and energy imports. The entire suite of models was authored and executed within the Python Jupyter environment.

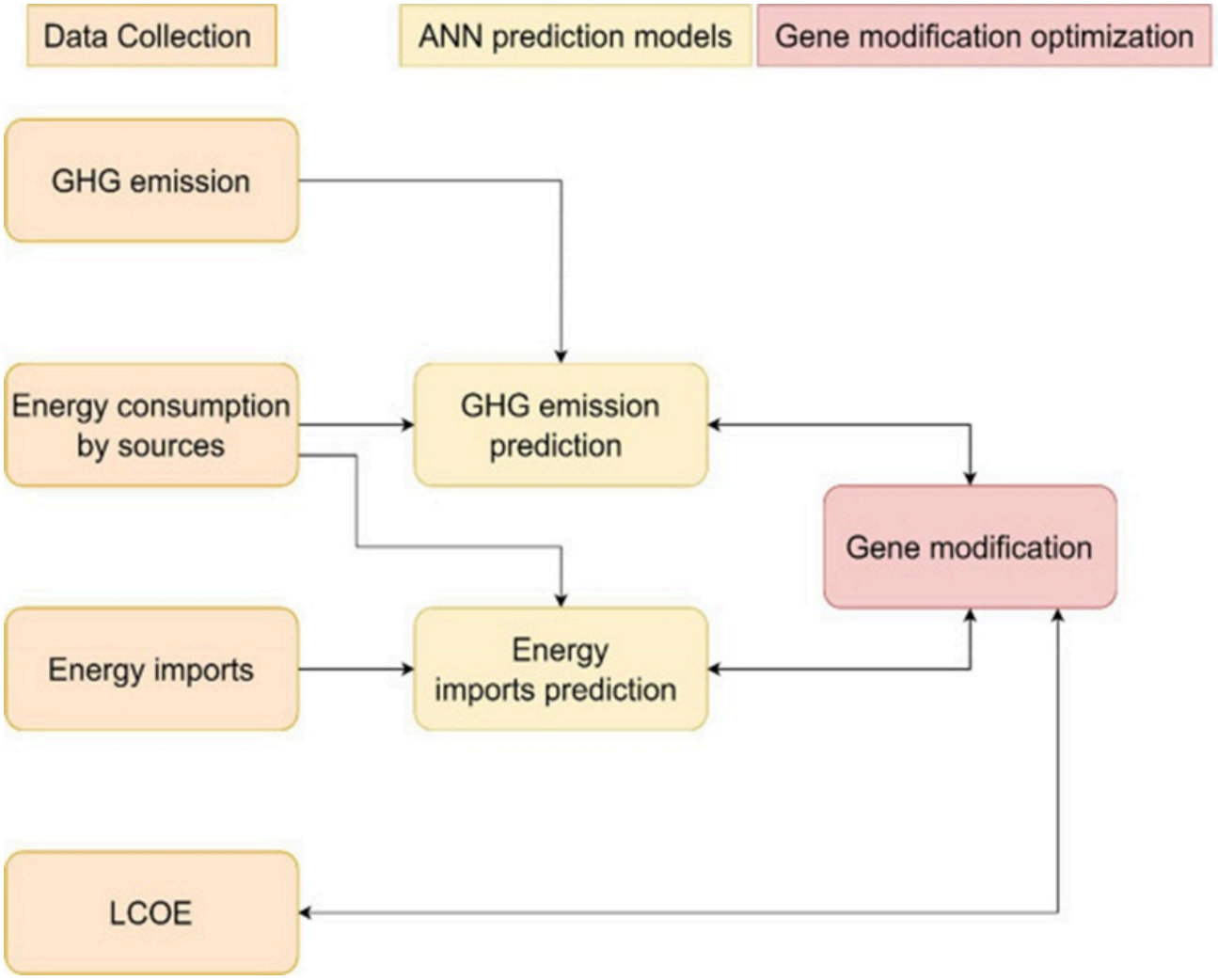

© 2023 The Author(s). | Published by Institute of Smart Energy Systems Press

Figure 1. Flowchart of the neural network GMOT for multi-objective energy resource management.

Data collection

Records about the European Union, covering energy consumption broken down by source, GHG emissions, LCOE, and energy imports, were sourced from a variety of repositories. Information on energy consumption by source and on GHG emissions was retrieved from the "Our World in Data" database, covering the years from 1965 up to 2021. The energy consumption by source dataset provides annual figures in terawatt-hours (TWh) across nine sources (Geo biomass, Biofuels, Solar, Wind, Hydro, Nuclear, Gas, Coal, and Oil). The GHG emissions dataset contains the yearly quantities of carbon dioxide, methane, and nitrous oxide released from all sources combined, expressed in metric tons. The energy imports dataset was obtained via the World Bank DataBank and reports, every year, the share of imported energy relative to overall energy consumption, for the period spanning 1965 to 2015. The levelized cost estimates attributed to geo biomass and biofuels were taken from a publication of the International Energy Agency (IEA) [46]. The LCOE values assigned to solar, wind, hydro, nuclear, gas, coal, and oil were, in turn, acquired from Brown and Foley [47]. **Table 1** offers a consolidated view of the datasets used in this study, along with the variables in each set, the corresponding units, the timeframe, and the originating sources. SI units are supplied in parentheses for each variable where such specification is appropriate.

Table 1. Summary of datasets, variables, units, time periods, and sources used in the study.

Dataset	Variable(s)	Measurement unit	Time span	Data source
Energy consumption by source	Geothermal, biomass, biofuels, solar, wind, hydropower, nuclear, natural gas, coal, and oil consumption	Terawatt-hours (TWh) *(3.6 × 1015 Joules)*	1965–2021	Our World in Data
GHG	Greenhouse gas (GHG) emissions	Metric tons *(1000 kg)*	1965–2021	Our World in Data
LCOE	Levelized Cost of Electricity (LCOE) corresponding to each energy source	US dollars per megawatt-hour (USD/MWh) *(2.78 × 10−7 Dollars per Joule)*	N/A	IEA [46]; Brown and Foley [47]
Energy imports	Imported energy volume	Percentage (%) of overall energy consumption	1965–2015	World Bank DataBank

Figure 2 depicts how energy consumption by source and GHG emissions have evolved across the EU between 1965 and 2021. Among the most notable patterns is the fact that oil and coal have long stood as the dominant contributors to energy consumption, reaching their respective zeniths around the 1970s and 1980s before entering a phase of broad-based contraction. Gas uptake has followed a path of consistent growth over the decades, whereas the role of nuclear energy has, in more recent times, stayed relatively unchanged. Energy streams classified as renewable—among them biofuels, solar, wind, and geothermal biomass—have registered step-by-step expansion. This trend mirrors a broader swing toward more ecologically sound energy practices. GHG emissions, for their part, have trended downwards since the opening years of the 1990s, a sign of deliberate action aimed at reducing the burden on the environment.

© 2023 The Author(s). | Published by Institute of Smart Energy Systems Press

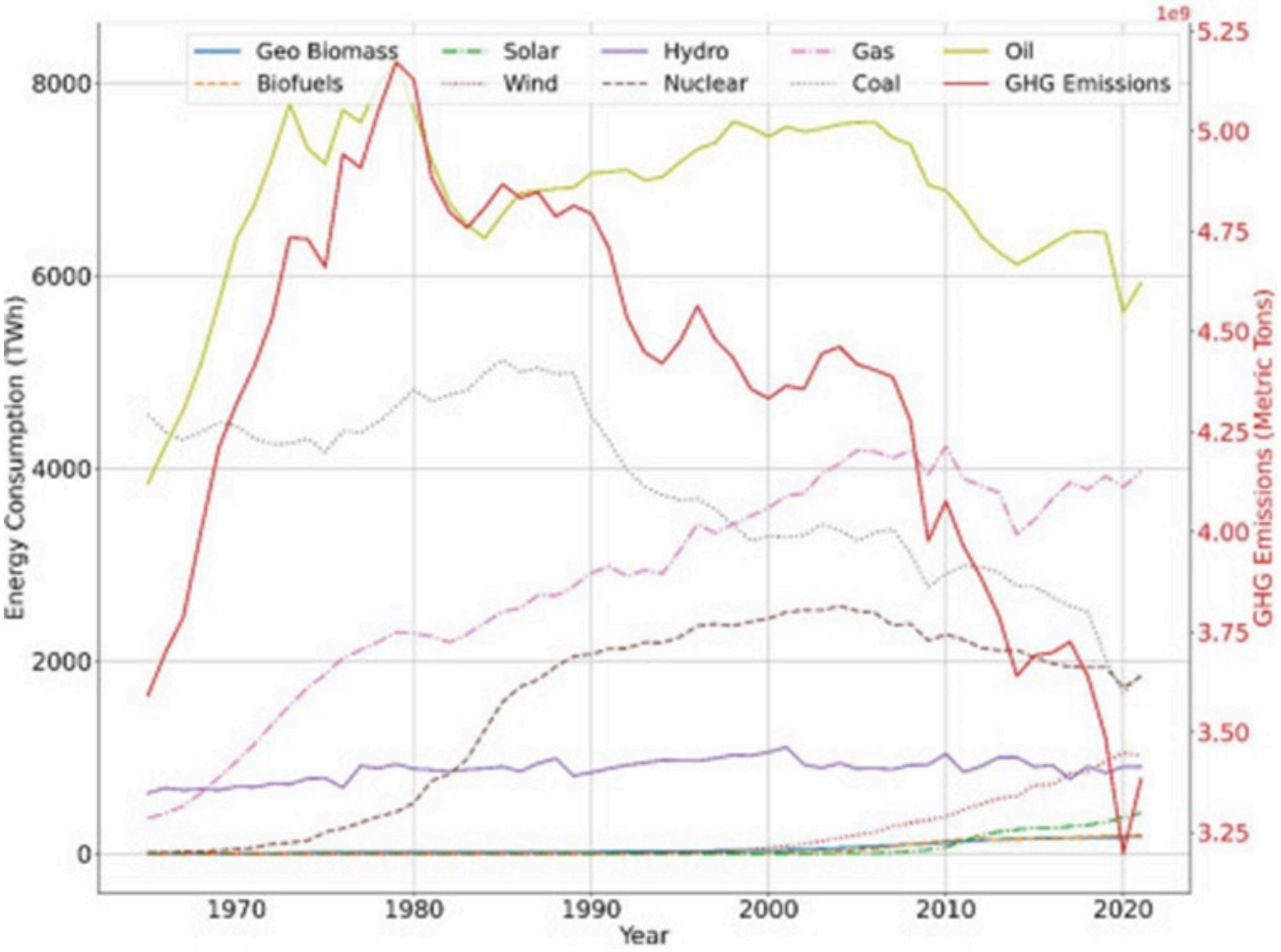

Figure 2. Trends in energy consumption and GHG emissions in the EU (1965–2021).

Figure 3 charts the course of energy imports as a proportion of total energy consumption across the EU from 1965 through 2015. Salient observations from this figure include a peak in energy imports near the end of the 1960s, when the ratio climbed beyond 54%. A substantial downturn in energy imports took hold from the late 1970s to the early 1980s, with the figure falling to around 44%. A progressive ascent in energy imports commenced in the late 1980s and gathered momentum throughout the 2000s, driving the metric to a renewed summit around 2008. Although the series exhibits oscillatory behaviour, the overarching tendency points toward a deepening reliance on imported energy over the past few decades.

© 2023 The Author(s). | Published by Institute of Smart Energy Systems Press

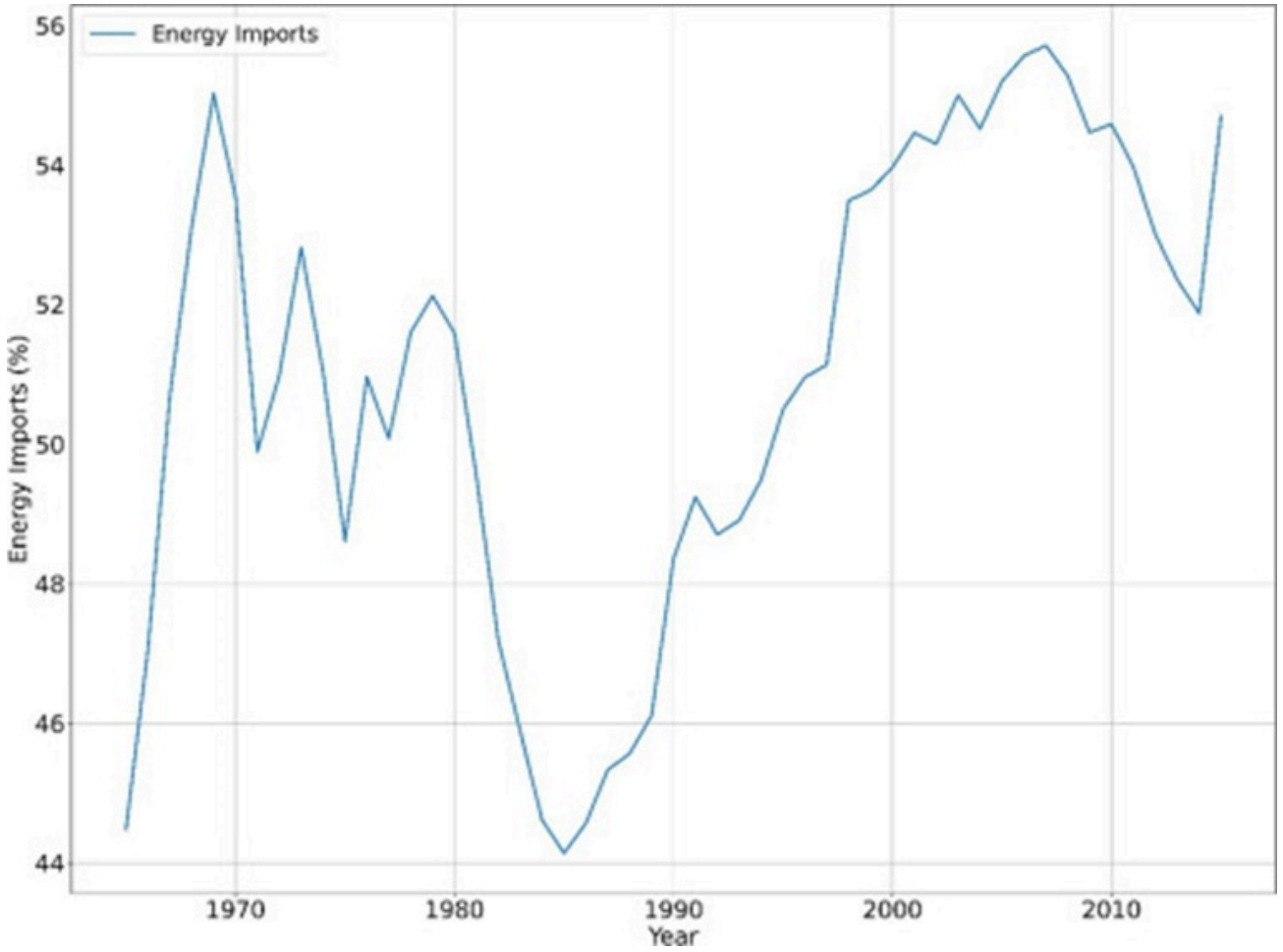

Figure 3. Trends in energy imports in the EU (1965–2015).

Artificial neural network (ANN)

A feedforward ANN architecture, using the Levenberg-Marquardt backpropagation algorithm, was deployed to train the two predictive models (one for GHG emissions and one for energy imports), as represented schematically in **Figure 4.**

© 2023 The Author(s). | Published by Institute of Smart Energy Systems Press

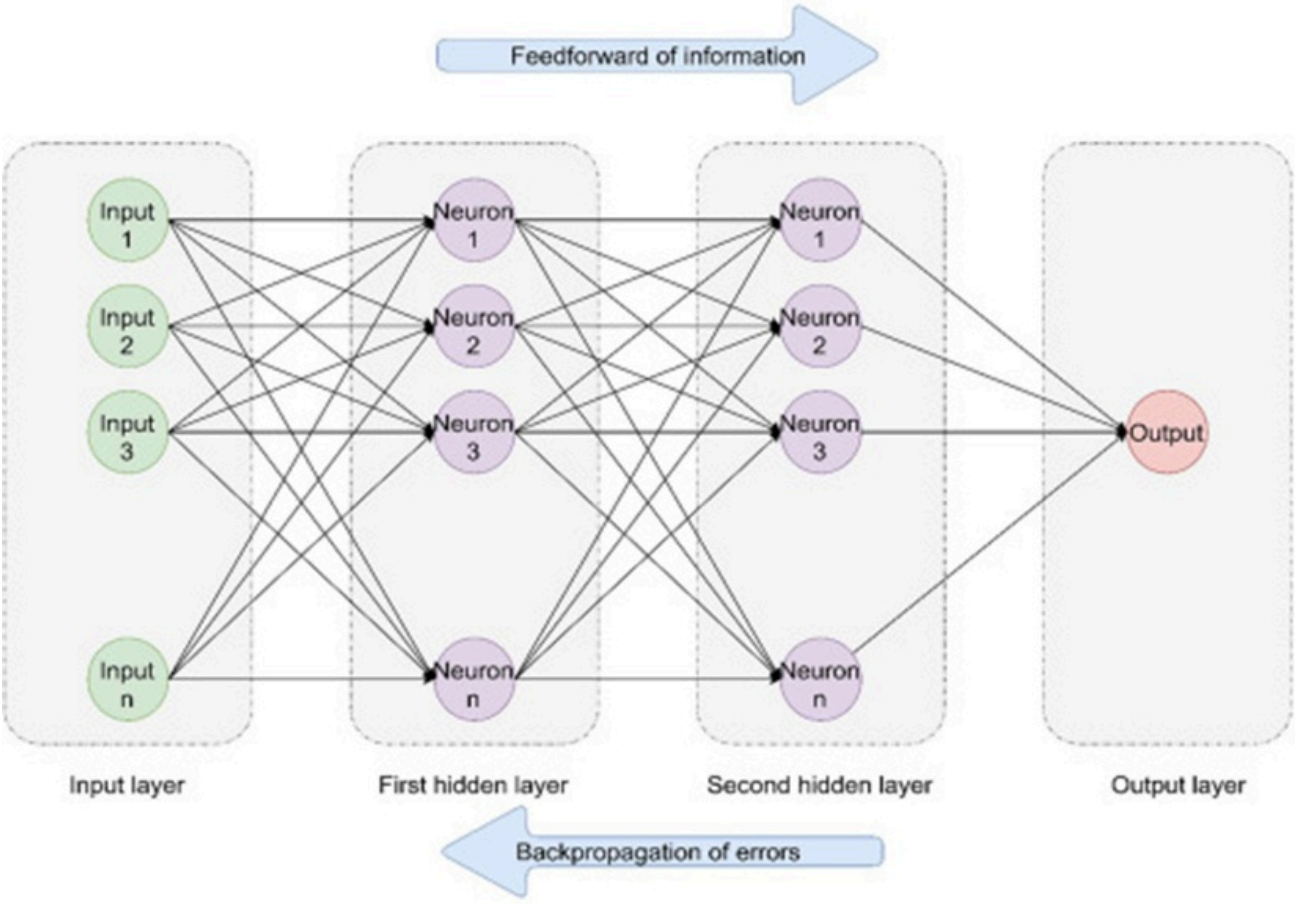

Figure 4. Architecture of neural network model with n inputs and one output.

Over the course of training, the supplied input data is pushed forward through the layered structure of the network in line with the equations stated below [48]:

$$a(1) = x \quad (1)$$

$$a(l) = \sigma(h(l)) \quad (2)$$

$$a(l) = \sigma(w(l-1)a(l-1) + b(l-1)) \quad (3)$$

The initial input vector x undergoes successive transformations as it propagates through the network, eventually yielding the output. For any given layer l, the activation vectors and the weighted input vectors are denoted by (l) and h(l), respectively, while the weight matrix w(l - 1) and the bias vector b(l - 1) serve as the connections between consecutive layers. The symbol σ denotes the activation function. Once the network output has been produced, the size of its error relative to the intended target is computed. At this point, the Levenberg-Marquardt algorithm steps in to update the weights and biases via backpropagation.

The delta rule is the tool used to work out the error attributable to each layer [49]:

$$\delta(L) = \nabla h(L) \mathscr{L} \odot \sigma'(h(L)) \quad (4)$$

© 2023 The Author(s). | Published by Institute of Smart Energy Systems Press

$$\delta(l) = ((w(l))T\delta(l+1)) \odot \sigma'(h(l)) \quad (5)$$

In the expression above, $\nabla h(L)\mathcal{L}$ stands for the gradient of the loss taken with respect to the network's output, the symbol $\odot$ denotes the operation of element-wise multiplication, and σ' represents the first derivative of the activation function. $\delta(L)$ corresponds to the error term associated with the output layer, while $\delta(l)$ refers to the error term at a given layer l, where l runs from 1 through to L - 1. The revision of weights and biases is carried out in accordance with the following rules [50]:

$$w^l := w^l - \Delta w^l \quad (6)$$

$$b^l := b^l - \Delta b^l \quad (7)$$

When considering layer l, the adjustment values for the weights and biases are derived based on regularized Gauss-Newton formulations. These formulations allow for a balance to be struck between the step direction characteristic of gradient descent and that characteristic of the Gauss-Newton method [48].

$$\Delta w^l = \left(J^T J + \lambda I\right)^{-1} J^T \delta^{l+1} \left(a^l\right)^T \quad (8)$$

$$\Delta b^l = \left(J^T J + \lambda I\right)^{-1} J^T \delta^{l+1} \quad (9)$$

In this context, Δw^l and Δb^l represent the update quantities applied to the weights and biases of layer l, respectively. The Levenberg-Marquardt parameter is denoted by λ, whereas the notation J is used for the Jacobian matrix. The Jacobian matrix itself is defined as follows [51]:

$$J_{ij}^{(l)} = \frac{\partial h_i^{(l)}}{\partial w_{ij}^{(l-1)}} \quad (10)$$

$$= \frac{\partial}{\partial w_{ij}^{(l-1)}} \left(\sum_k w_{ik}^{(l-1)} a_k^{(l-1)} + b_i^{(l-1)} \right) \quad (11)$$

$$= a_j^{(l-1)} \quad (12)$$

$$\delta^{(L)} = J^{(L)} \left(f\left(h^{(L)}\right) - y \right) \quad (13)$$

$$\delta^{(l)} = \left(J^{(l)}\right)^T \left(J^{(l)} \left(J^{(l)}\right)^T + \mu I \right)^{-1} \delta^{(l+1)} \quad (14)$$

$$\frac{\partial E}{\partial w_{ij}^{(l)}} = a_j^{(l-1)} \delta_i^{(l)} \quad (15)$$

$$\frac{\partial E}{\partial b_i^{(l)}} = \delta_i^{(l)} \quad (16)$$

© 2023 The Author(s). | Published by Institute of Smart Energy Systems Press

The error vector for the output layer is denoted by $\delta^{(L)}$. The Jacobian matrix specific to layer l is shown as $J^{(l)}$. A regularization parameter, labelled μ, controls the size of the update step. The symbol I denotes the identity matrix. The computation of the derivative of the cost function with respect to the weights and biases is executed as outlined below [51]:

$$\frac{\partial E}{\partial w_{ij}^{(l)}} = \frac{\partial E}{\partial h_i^{(l)}} \frac{\partial h_i^{(l)}}{\partial w_{ij}^{(l)}} \quad (17)$$

$$= \delta_i^{(l)} a_j^{(l-1)} \quad (18)$$

$$\frac{\partial E}{\partial b_i^{(l)}} = \frac{\partial E}{\partial h_i^{(l)}} \frac{\partial h_i^{(l)}}{\partial b_i^{(l)}} \quad (19)$$

$$= \delta_i^{(l)} \quad (20)$$

During each iteration, the weights and biases are refreshed by applying the rules that follow [51]:

$$w_{ij}^{(l)} := w_{ij}^{(l)} - \eta \frac{\partial E}{\partial w_{ij}^{(l)}} \quad (21)$$

$$b_i^{(l)} := b_i^{(l)} - \eta \frac{\partial E}{\partial b_i^{(l)}} \quad (22)$$

The learning rate, designated by the symbol η, controls the magnitude of the changes applied to the weights and biases. The entire algorithm is applied in a loop until either the error converges to a steady value or the upper limit placed on the number of epochs is reached.

As has been detailed above, a feedforward ANN underpinned by Levenberg-Marquardt backpropagation was brought into service (**Eqs. 1–22**) to generate predictions of GHG emissions and energy imports from the consumption figures of different energy sources. By systematically experimenting with a variety of hyperparameter combinations, the algorithm can identify the most favourable setup and, in doing so, improve the model's overall performance. **Table 2** lays out the ANN parameter values that were put to the test: the number of inputs, the number of outputs, the number of hidden layers together with their neurons, the maximum permitted number of epochs, the maximum training duration, the performance goal, the learning rate, the activation function, and the cross-validation scheme.

Table 2. Hyperparameter values and descriptions for neural network optimization.

Parameter	Description	Values evaluated during ANN optimization
Input variables	Total number of variables supplied to the network as inputs	9
Output variables	Number of predicted target variables generated by the network	1
Hidden layers	Count of hidden layers incorporated in the ANN architecture	2–10

© 2023 The Author(s). | Published by Institute of Smart Energy Systems Press

Hidden neurons	Number of neurons assigned to each hidden layer	2–10
Maximum epochs	Maximum training cycles allowed before terminating the learning process	1000
Performance target	Lowest desired Mean Squared Error (MSE) value	0
Learning rate	Positive coefficient determining the speed of weight adjustment in response to prediction error	0.001, 0.01, 0.1
Activation function	Function applied within hidden layers to introduce nonlinearity	'relu', 'tanh'
Cross-validation	Number of folds employed in the grid-search cross-validation procedure	5

Gene modification optimization technique (GMOT)

This portion of the study is dedicated to the design of a novel gene modification approach intended to cope with the parallel optimization of multiple objectives that stand in opposition to one another. The gene modification procedure introduced here is geared toward sharpening both the exploratory capacity and the convergence behaviour of the multi-objective optimization routine when faced with contradictory aims.

Gene representation

The starting point is to carefully select a gene representation format that is well matched to the specificities of the problem domain. The chromosomal structure is built up from n individual genes, each of which takes its value from the continuum of real numbers and is stored as a floating-point quantity. In the context of optimizing the nine distinct sources of energy consumption across the EU, the chromosome is composed of exactly nine genes, with each gene encoding the magnitude of one particular energy consumption source, as shown in **Figure 5.**

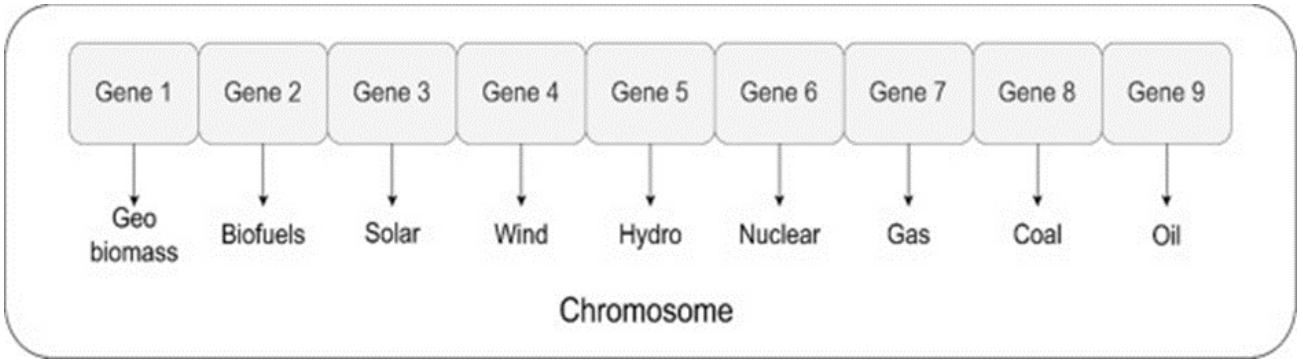

Figure 5. Representation of gene sequence in the optimization process.

Objective selection

The first task when formulating a fitness function is to single out and settle on the objectives that shape the optimization problem [52]. Since the aim of this work is to drive down GHG emissions, expenses (LCOE), and energy imports by adjusting the nine energy consumption sources, three standalone fitness functions are required, each encompassing nine genes. The trained ANN models were used to produce estimates of GHG emissions and energy imports corresponding to

© 2023 The Author(s). | Published by Institute of Smart Energy Systems Press

assorted consumption mixes across the nine energy sources. The associated costs were calculated by taking the volume of each energy source, multiplying it by the source's respective LCOE, and then aggregating all resulting products.

GMOT algorithm

Figure 6 lays out the operational sequence of the GMOT algorithm. The subsections that follow unpack each phase of the GMOT routine.

© 2023 The Author(s). | Published by Institute of Smart Energy Systems Press

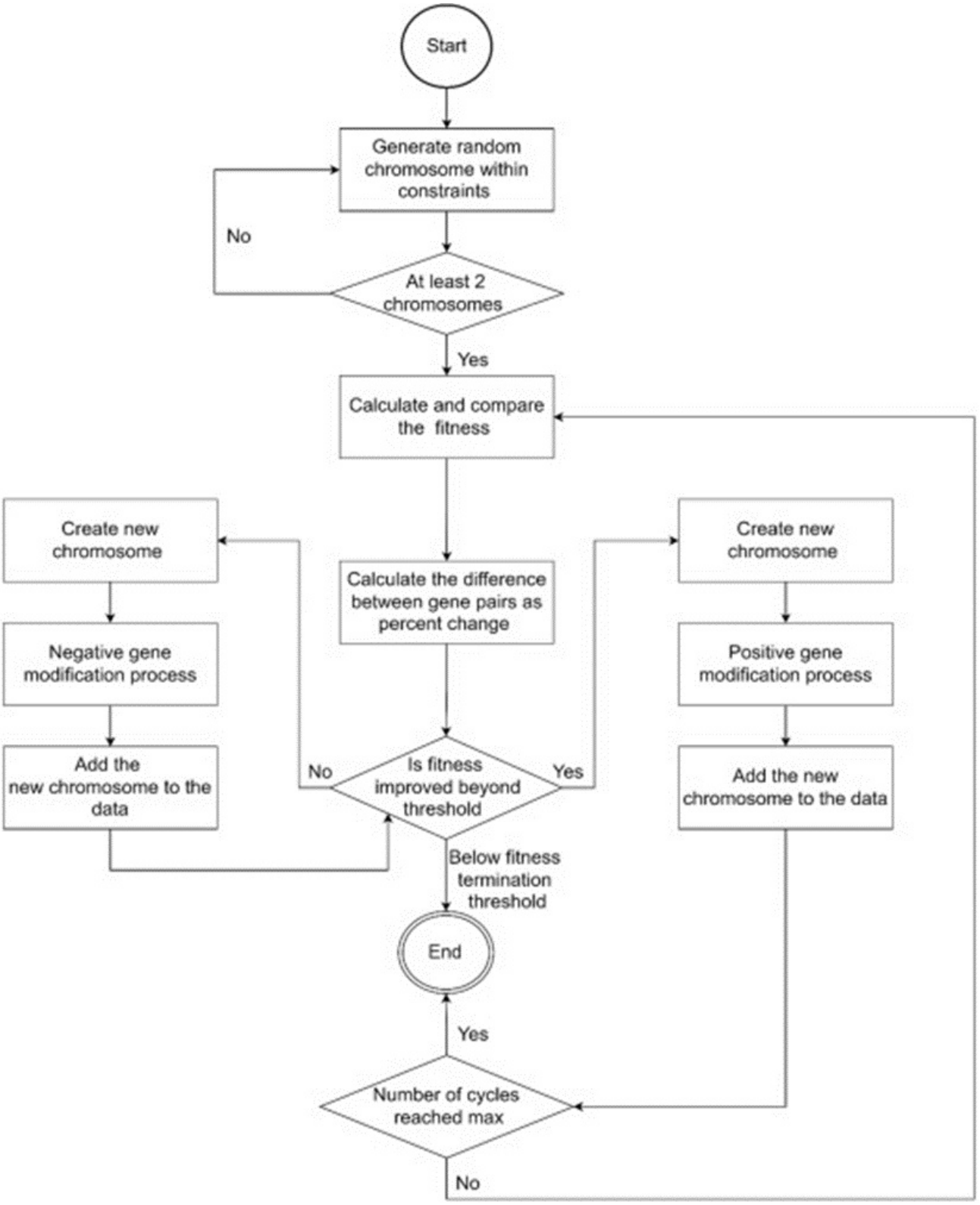

Figure 6. Neural network-enhanced gene modification optimization algorithm workflow.

Initialization and chromosome generation

© 2023 The Author(s). | Published by Institute of Smart Energy Systems Press

The routine is launched by randomly constructing an initial collection of candidate gene configurations, each one compliant with the energy demand restrictions. Those restrictions were built around an assumed annual growth rate [53]. Because the initialization phase generates only a single chromosome at first, a second chromosome is created identically to serve as a point of reference. In this way, two random chromosomes come into existence side by side. With the benchmark now in place, the algorithm shifts into the objective assessment stage, in which the fitness of each chromosome is gauged against its immediate predecessor.

Fitness evaluation

A complication arises when attempting to judge the fitness of the objective functions attached to the two chromosomes, because each fitness function is expressed in its own units and operates on its own scale. It is simply not practicable to put functions with unlike measures and magnitudes side by side in a direct comparison. Resorting to normalization does not solve the issue, given that GHG emission figures and LCOE values can shift dramatically based on the ANN-generated projections, meaning that the upper and lower extremes remain indeterminate. A workaround was fashioned in the form of an average percentage of improvement. With this approach, the percentage improvement—understood here as the percentage reduction in the three objective functions linked to a given chromosome—is compared against the value from the preceding iteration or generation, as formalized in **Eqs. 23–25**. In these expressions,F_1, F_2, and F_3 designate the first, second, and third objective function fitness values belonging to a chromosome c, while i marks the position of the current iteration inside the GMOT sequence.

$$Percent\ improvement\ of\ F_{1(c)} = \frac{F_{1(i)} - F_{1(i-1)}}{F_1(i-1)} * 100\% \quad (23)$$

$$Percent\ improvement\ of\ F_{2(c)} = \frac{F_{2(i)} - F_{2(i-1)}}{F_2(i-1)} * 100\% \quad (24)$$

$$Percent\ improvement\ of\ F_{3(c)} = \frac{F_{3(i)} - F_{3(i-1)}}{F_3(i-1)} * 100\% \quad (25)$$

The mean improvement across the three objective functions $F_{1(c)}$, $F_{2(c)}$ and $F_{3(c)}$ for each chromosome c is subsequently computed in accordance with **Eq. 26.**

$$Total\ Percent\ improvement\ for\ chromosome\ (c) = \frac{F_{1(c)} + F_{2(c)} + F_{3(c)}}{3} \quad (26)$$

Gene comparison

The next stage entails calculating the discrepancy between every matching gene pair and expressing that discrepancy as a percentage. Undertaking this calculation is critical for arriving at a rigorous quantification of the gap or degree of dissimilarity between genes. The percentage differences that emerge from this operation act as informative metrics that will be exploited in the phases still to come, enabling head-to-head comparison and a full appraisal of gene-level variation. These metrics are destined to play a pivotal role in guiding choices about gene modification tactics.

As the earlier steps have shown, the initialization routine delivers two chromosomes produced at random. From that point forward, each successive iteration produces a newly altered chromosome, one that carries the potential to match or surpass the fitness of the chromosome that came directly before it. During the gene comparison step, a percentage is calculated, following **Eq. 27,** for each pair of genes drawn from the two chromosomes (the chromosome of the current iteration c and the chromosome of the previous iteration c - 1). This equation is run over the full set of genes (g)

© 2023 The Author(s). | Published by Institute of Smart Energy Systems Press

(spanning from g = 1 through to 9), thereby yielding nine percentage values that can fall anywhere inside the range from -100% to 100%.

$$Percentage\ difference\ in\ Gene\ pair_g = \frac{Gene_g(c) - Gene_g(c-1)}{Gene_g(c-1)} * 100\% \quad (27)$$

Gene modification process

After the nine gene-pair differences have been determined, the algorithm embarks on a gene modification operation whose direction is dictated by the fitness level of the newest chromosome. Specifically, the algorithm will either execute a positive gene modification routine if the fitness of chromosome c is better than that of chromosome c-1, or a negative gene modification routine if the fitness of chromosome c is worse than that of chromosome c-1. If the two chromosomes have fitness scores whose gap is smaller than a set threshold, a counter is activated. If the fitness fails to improve for 15 chromosomes (iterations) in a row beyond that threshold, the whole procedure is terminated, and the gene combination that yielded the best result for the problem under study is output.

Positive gene modification process:

Whenever the fitness of chromosome c exceeds the fitness of the chromosome that preceded it (c - 1), the positive gene modification routine commences by initializing a blank, newly created chromosome that houses nine genes. The percentages obtained via **Eq. 27** are then taken and multiplied by the matching gene value belonging to chromosome c. The product of this multiplication is subsequently added onto the original gene value, as stipulated in **Eq. 28.**

$$Modified\ Gene_g = (Percentage\ difference\ in\ Gene\ pair_g * Gene_g) + Gene_g \quad (28)$$

This sequence of actions is repeated for every gene pair, giving rise to nine altered genes, which are then slotted into the newly assembled chromosome.

Negative gene modification process:

Whenever the fitness of chromosome c does not beat (i.e., is poorer than) the fitness of chromosome c - 1, a negative gene modification routine is set in motion by opening a new, empty chromosome equipped with nine genes. The percentages derived through **Eq. 27** are multiplied by a hyperparameter (hp) and by the matching gene value taken from chromosome c. The result of this multiplication is then subtracted from the gene value, as laid down in **Eq. 29.**

$$Modified\ Gene_g = (Percentage\ difference\ in\ Gene\ pair_g * hp * Gene_g) - Gene_g \quad (29)$$

The selection of the hyperparameter follows a logic of incremental adjustment. Each time the addition of a new chromosome brings about a decline in fitness, the algorithm undertakes a cautious reversal equal to a 0.6 step size, rather than undoing an entire step back to the previous iteration. This approach sharpens the course of optimization and progressively dials in the best chromosome. The entire set of operations is carried out for each gene pair, generating nine modified genes that are incorporated into the new chromosome.

Constraints

The optimization formulation includes constraints, the principal one being that the total of all genes must represent the energy growth contributed by every source taken together. In addition, each gene (which corresponds to a particular energy source) is required to remain within designated upper and lower cutoffs. Because modified genes could take on values that run afoul of these limits, the gene modification apparatus is engineered to ensure that the sum across all genes will, without exception, equal the prescribed figure (annual energy consumption in the present case).

© 2023 The Author(s). | Published by Institute of Smart Energy Systems Press

The gene modification procedure enforces compliance with the problem's constraints through two separate control mechanisms. To begin with, determining the percentage difference between each gene pair—as performed through **Eq. 27**—keeps the resultant percentage difference within the corridor bounded by -100% and 100%. It is worth underlining that the summation of all these percentage differences invariably adds up to zero, a property that upholds the stipulated constraints and leaves the total sum of genes inside every chromosome unchanged. Furthermore, any gene modification that would push a value beyond the upper boundary triggers an adjustment protocol; at that moment, the gene value is forcibly pegged to the maximum level allowed by the upper boundary. Any surplus amount apportioned to that gene is reassigned to the gene that currently holds the smallest value. In the reverse situation, if a gene's value falls short of the lower boundary after modification, the gene value is reset to the lowest permissible level specified by the lower boundary for that gene. The excess quantity that would have been allocated to this gene is deducted from those genes that occupy the higher end of the value spectrum. The containment procedure sketched above, which bears a resemblance to a mutation-like operator, accomplishes two things at once: it enlarges the sweep of the solution-space search. It diminishes the likelihood of genes becoming trapped at either their ceiling or floor values. By deploying these twin regulatory mechanisms, the problem preserves its structural consistency while opening the door to a vigorous examination of the solution landscape.

Once the gene modification stage draws to a close, a single full iteration has been wrapped up. At this fork, the algorithm takes one of two routes: it either halts operations if the tally of iterations has gone beyond a predetermined ceiling (specifically, 1000 chromosomal iterations), or it circles back and repeats the sequence until 15 successive gene modifications yield fitness values that sit below the designated threshold. This self-adjusting logic delivers efficient convergence toward the most favourable outcomes while leaving room for distinct stopping conditions.

Performance metrics

At the close of each generational cycle, the fitness belonging to the various functions undergoes computation. Bringing the fitness scores onto a level playing field for unbiased juxtaposition and synthesis calls for a vital normalization step. Because the set of three fitness functions operates within separate units and across dissimilar magnitude ranges, normalizing them is essential if one hopes to arrive at a steady, directly comparable yardstick that spans the chromosomal generations (iterations) under examination. For this paper, the min-max normalization formula was deployed in line with the descriptions offered by **Eqs. 30-32**. An important detail to note is that this normalization operation is held back until the algorithm has fully concluded, at which point the complete set of values is known.

$$NF_1 = \frac{F_{1c} - \min(F_1)}{\max(F_1) - \min(F_1)} \quad (30)$$

$$NF_2 = \frac{F_{2c} - \min(F_2)}{\max(F_2) - \min(F_2)} \quad (31)$$

$$NF_3 = \frac{F_{3c} - \min(F_3)}{\max(F_3) - \min(F_3)} \quad (32)$$

In these equations, NF_1 , NF_2 , and NF_3 denote the normalized counterparts of the fitness functions F_1, F_2 , and F_3, evaluated sequentially for c = 1 up to the final chromosome in the series.

What follows is the calculation of the plain mean taken over all the normalized fitness readings for the trio of distinct functions, as spelled out in **Eq. 33.** The resulting average figure doubles as an all-encompassing indicator of performance, capturing under a single number the combined effectiveness delivered by the three functions. Under ideal circumstances, an average reading of 0 would represent the best achievable outcome, in keeping with the study's goal of

© 2023 The Author(s). | Published by Institute of Smart Energy Systems Press

pressing the fitness functions down to their lowest possible level. By contrast, a score of 1 would indicate the poorest output emerging from the fitness functions.

$$Avgerage\ Fitness\ =\ Average(NF_1, NF_2, NF_3) \quad (33)$$

Over the course of this investigation, a pair of long-established distance measures—namely Euclidean Distance and Normalized Euclidean Distance—were used to gauge and compare their performance during the optimization sequence in relation to the GMOT. Euclidean Distance, for its part, measures the direct straight-line separation between a pair of data points situated in a multi-dimensional space. In this application, it focuses on ascertaining the gap between the fitness coordinates and the origin point (0,0,0) [54]. Its value is obtained through **Eq. 34:**

$$Euclidean\ Distance\ =\ \sqrt{F_1{}^2 + F_2{}^2 + F_3{}^2} \quad (34)$$

The Normalized Euclidean Distance variant is particularly relevant in this context because it incorporates the normalized figures tied to each fitness function. This yields a standardized benchmark suited to appraising dissimilarity inside a multi-dimensional framework [55]. The Normalized Euclidean Distance is computed via **Eq. 35:**

$$Normalized\ Euclidean\ Distance\ =\ \sqrt{NF_1{}^2 + NF_2{}^2 + NF_3{}^2} \quad (35)$$

Results and Discussion

To forecast GHG emissions, the combination of parameters yielding the best performance was identified through a grid search **(Table 2)**. The ANN was configured with a pair of hidden layers, each furnished with five nodes, adopted the ReLU activation function, and ran at a learning rate of 0.001. This setup delivered an R-squared score of 0.97. For the analogous task of predicting energy imports, a comparable configuration was chosen, featuring two hidden layers populated by four nodes apiece, which culminated in an R-squared score of 0.85.

Using the 2021 records, the GMOT algorithm was tested against real-world statistics on energy consumption, LCOE, GHG emissions, and energy imports. When the algorithm's best proposed recommendations were set alongside the observed 2021 data, the gap between the two underscored the prospective advantages locked within the algorithm's suggestions—prominently, reductions in LCOE, a drop in energy imports, and a contraction in GHG emissions.

Key findings

The collection of energy consumption levels that the GMOT trialed for every energy source (gene) across multiple generations/iterations is laid out in **Figure 7**. The chart spotlights four critical reference points: the initial value produced at random, the maximum reading ever explored, the minimum reading ever explored, and the ultimate optimum value that was settled upon. The optimization routine was bounded to generate outputs that remained both practical and plausible; the ceiling placed on overall energy expansion was fixed at 824 TWh, a figure that mirrors the year-on-year increment in energy consumption experienced during 2021. Each distinct energy source was free to fluctuate anywhere between 0 and 824 TWh, thereby allowing considerable latitude in how the total was parcelled out.

© 2023 The Author(s). | Published by Institute of Smart Energy Systems Press

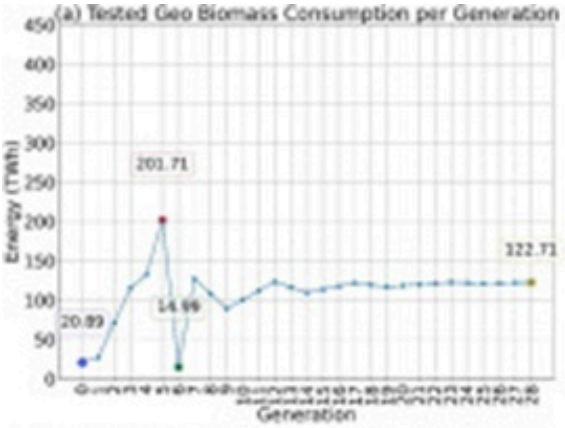

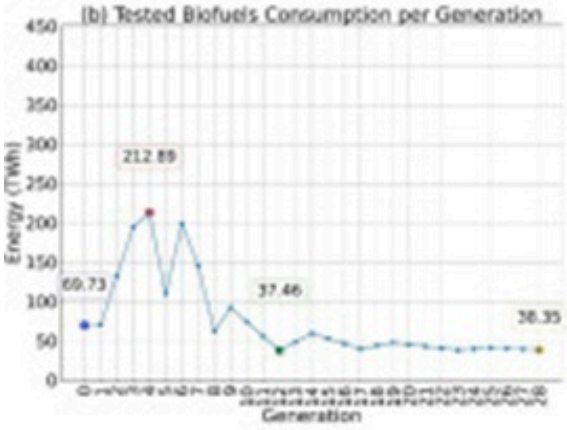

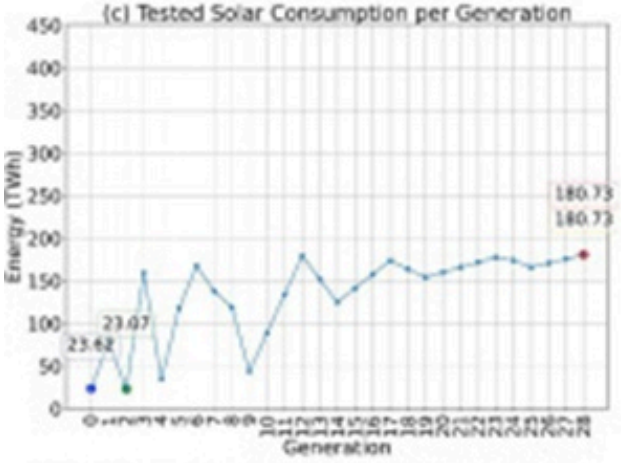

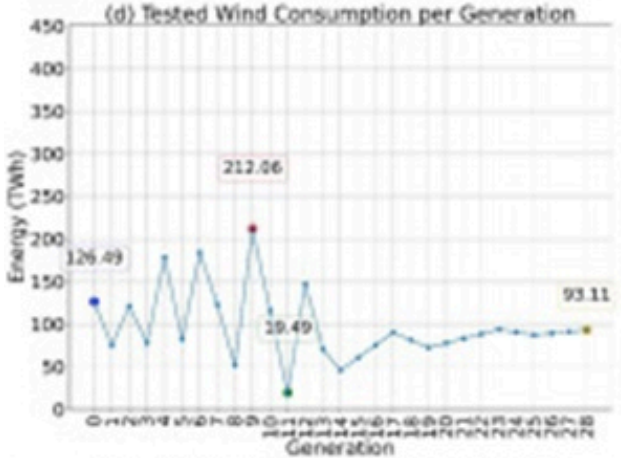

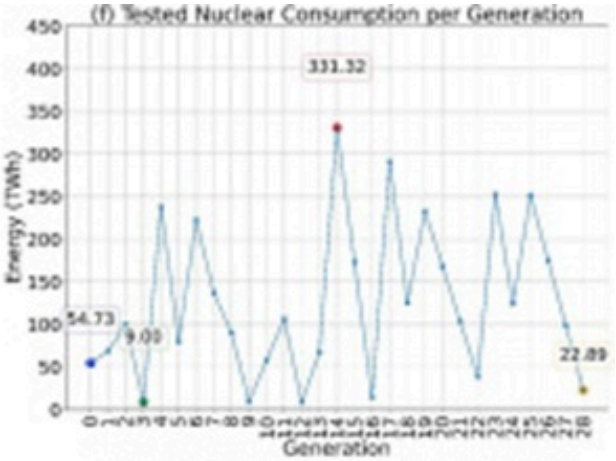

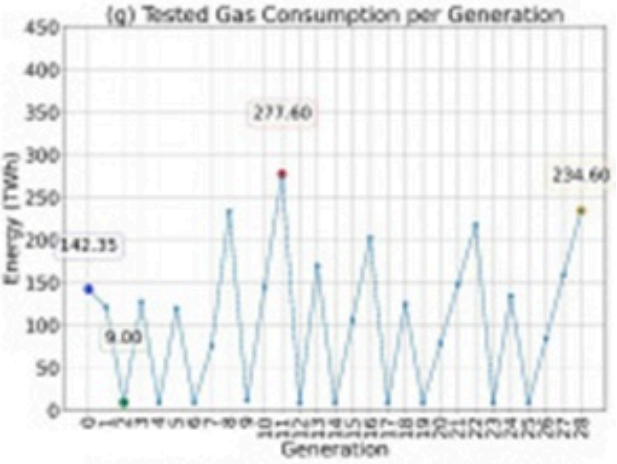

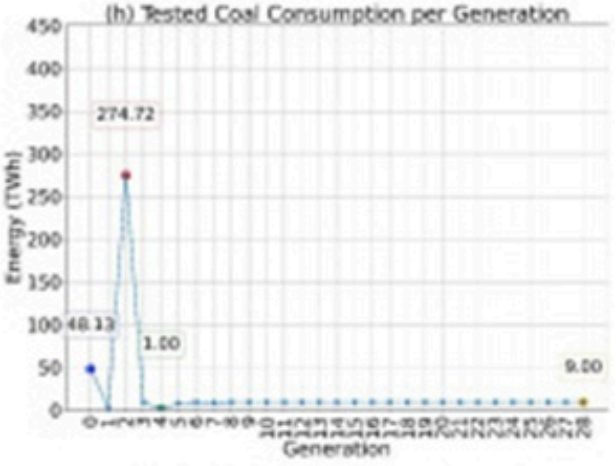

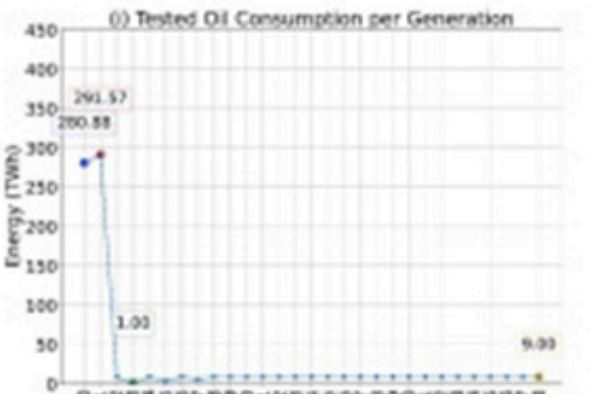

© 2023 The Author(s). | Published by Institute of Smart Energy Systems Press



of approximately 23.62 TWh to 180.73 TWh, a jump that captures the momentum gathering behind renewable, low-emitting energy forms. When wind energy is considered, the range of trial readings extended from an initial random setting of 126.49 TWh to an optimized endpoint of 93.11 TWh, with the overall band of exploration running from 19.49 TWh to 212.06 TWh. For hydro, the figures moved from 57.18 TWh to an optimized 113.67 TWh, hinting at a stronger reliance being placed on this renewable stream. Nuclear power, by contrast, underwent dramatic oscillations, registering anywhere from 54.73 TWh to a high of 331.32 TWh, before the search ultimately homed in on a value of 22.89 TWh. Gas transitioned from 142.35 TWh up to a recorded peak of 277.60 TWh and finally settled at an optimized figure of 234.60 TWh. Coal underwent a compression from 48.13 TWh down to just 9 TWh, even though the search had once probed as high as 274.72 TWh; oil followed a similar trajectory, receding from 280.88 TWh to an optimized 9 TWh, having reached an upper tested limit of 291.57 TWh.

Within the bounds of this study, the GMOT sequence came to a close at the optimum value during the 28th generation. This indicates that one among the stopping rules established beforehand was triggered at this generation (more precisely, the criterion specifying 15 successive generations for which the overall pace of enhancement fell short of the pre-set termination threshold). Such an outcome verifies that the generational trajectory of optimization had entered a plateau phase. The best solution produced by the GMOT was associated with an average fitness value of 0.26 (as per **Eq. 33**). When interpreted within the setting of the multi-objective genetic algorithm utilized in this research, this outcome signals a close approach toward the theoretically ideal solution. The result reinforces the strength of the algorithm, given that the uncovered solution sits within close range of the optimal resolution existing in the multi-objective trade-off terrain.

Figure 8 presents a side-by-side view of the factual energy consumption totals against those produced by the optimization for the EU energy sources in the year 2021. The empirical consumption breakdown shows the dominant share belonging to oil (5922 TWh), followed in order by gas (3966 TWh), coal (1871 TWh), nuclear (1838 TWh), wind (1019 TWh), hydro (901 TWh), solar (420 TWh), biofuels (189 TWh), and, finally, geo biomass (180 TWh). The rebalanced consumption profile, as dictated by the Gene Modification Optimization Technique, calls for enlargements on the order of 62.6% for geo biomass, 18.2% for biofuels, 32.5% for solar, 11.5% for wind, 12.7% for hydro, and 1.8% for gas. Running counter to those increases, GMOT prescribes a pullback of 5% for nuclear, 10.9% for coal, and 4.9% for oil, a set of recommendations that marks a deliberate turn toward energy sources that are more sustainable and renewable, while simultaneously loosening the grip of fossil fuels.

© 2023 The Author(s). | Published by Institute of Smart Energy Systems Press

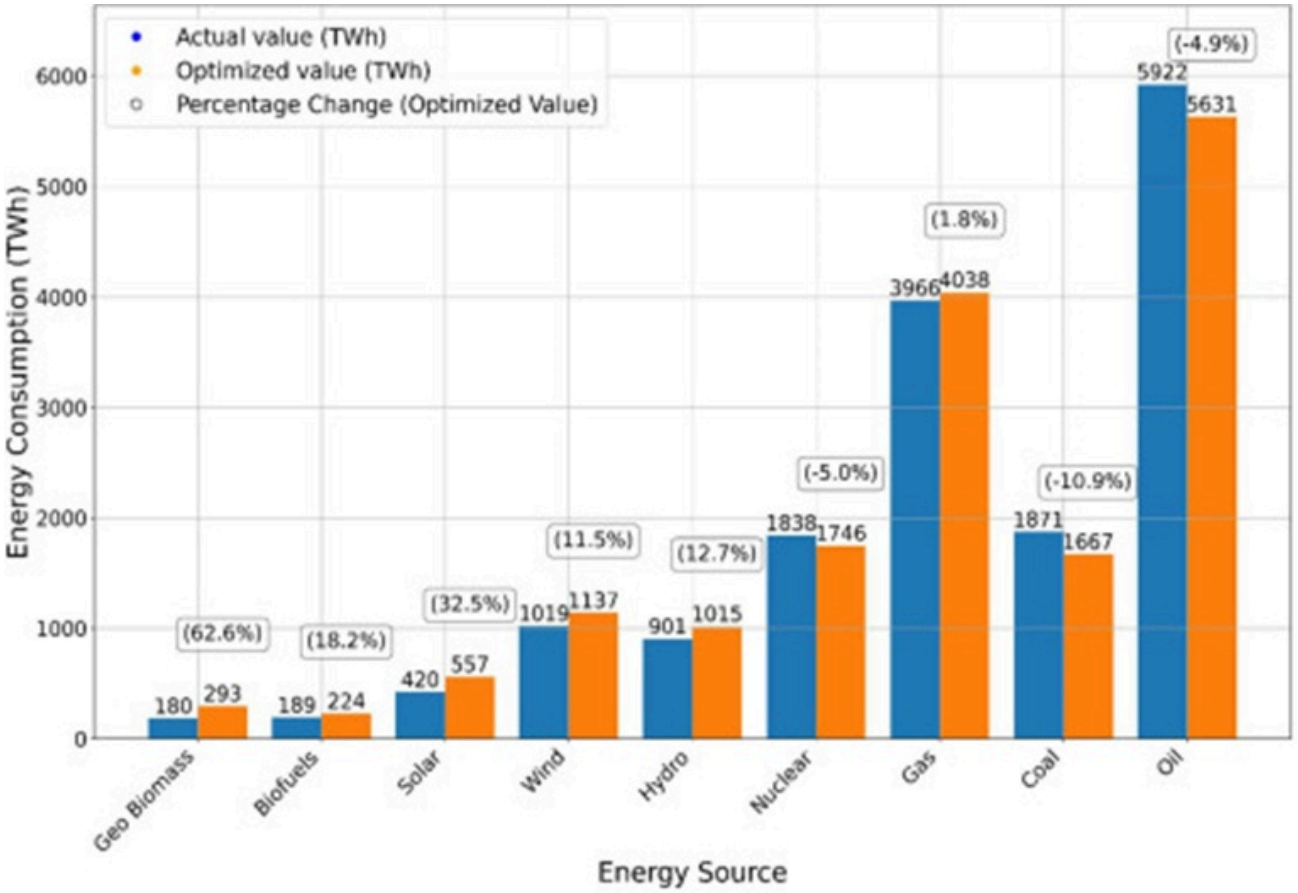

Figure 8. Comparison of actual and simulated optimized energy consumption by source in the EU for the year 2021.

The optimization results displayed in **Figure 8** cast light on the potency of the GMOT as a tool for remolding the energy landscape. By endorsing steep rises for geo biomass, solar, wind, and hydro, the GMOT assigns clear priority to scaling up locally sourced, renewable energy streams. A reorientation of this nature not only dovetails with ecological sustainability objectives by reducing greenhouse gas emissions but also diminishes the degree to which the EU must lean on foreign energy supplies, thereby reinforcing the bloc's energy security posture. The winding down of conventional fossil-based sources—coal, oil, and nuclear energy—brings additional emphasis to the role played by GMOT in compressing the environmental burden tied to EU energy consumption patterns. The comparatively slight 1.8% bump in gas usage implies that it is being positioned as a transitional component within the broader energy mix.

Taken together, these outcomes corroborate GMOT's ability to propel the EU's twin ambitions of energy efficiency and sustainability, while also revealing its considerable potential for extensive application in global energy resource optimization. The technique's ability to interweave and balance multiple objectives—cost containment, emissions control, and import minimization—constitutes a noteworthy stride forward in the repertoire of energy optimization methodologies.

Figure 9 illustrates the trajectory of the energy import indicator, expressed as a fraction of total energy consumption, across the succession of generations produced by the GMOT algorithm. In the earliest generations, wide oscillations are evident, with the import share climbing to a maximum of 60.50%. As the optimization march presses forward, however, the algorithm progressively converges on a more settled reading. The best energy import figure is located at 58.45%, which amounts to a slender increase of 2% relative to the baseline level. This modest expansion implies that, even as certain objectives—prominently cost and GHG emissions—register considerable improvements, the optimized energy composition demands a minor uptick in import volumes. A trade-off of this kind could plausibly arise from the need to

© 2023 The Author(s). | Published by Institute of Smart Energy Systems Press

complement indigenous renewable energy supplies with dependable, potentially imported, low-GHG energy carriers to safeguard a continuous and stable energy flow.

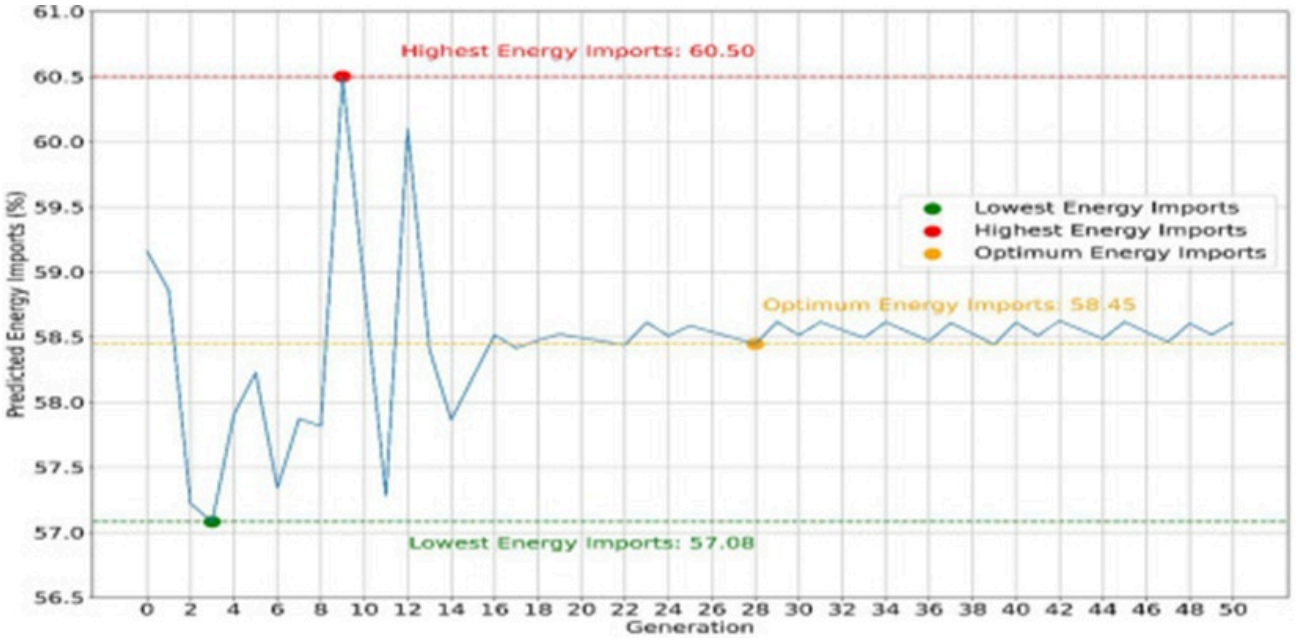

Figure 9. Energy imports as a percentage of total energy consumption across generations.

Figure 10 tracks how the cost metric, quantified via the Levelized Cost of Energy (LCOE), evolves from one generation to the next throughout the GMOT optimization sequence. The peak recorded cost sits close to $142,129,141, a number that mirrors the early-stage, randomly assigned values. With the passage of generations, the GMOT routine progressively squeezes the LCOE lower, ultimately locking in an optimal cost of $77,916,061 when generation 28 arrives. This outcome amounts to a hefty contraction of roughly 46% when set beside the original cost baseline. Such sweeping financial savings highlight GMOT's promise to boost the economic attractiveness of energy sources, strengthening their competitive position. The manner in which cost readings level off during the closing generations testifies to the algorithm's proven knack for recurrently homing in on cost-efficient energy blueprints.

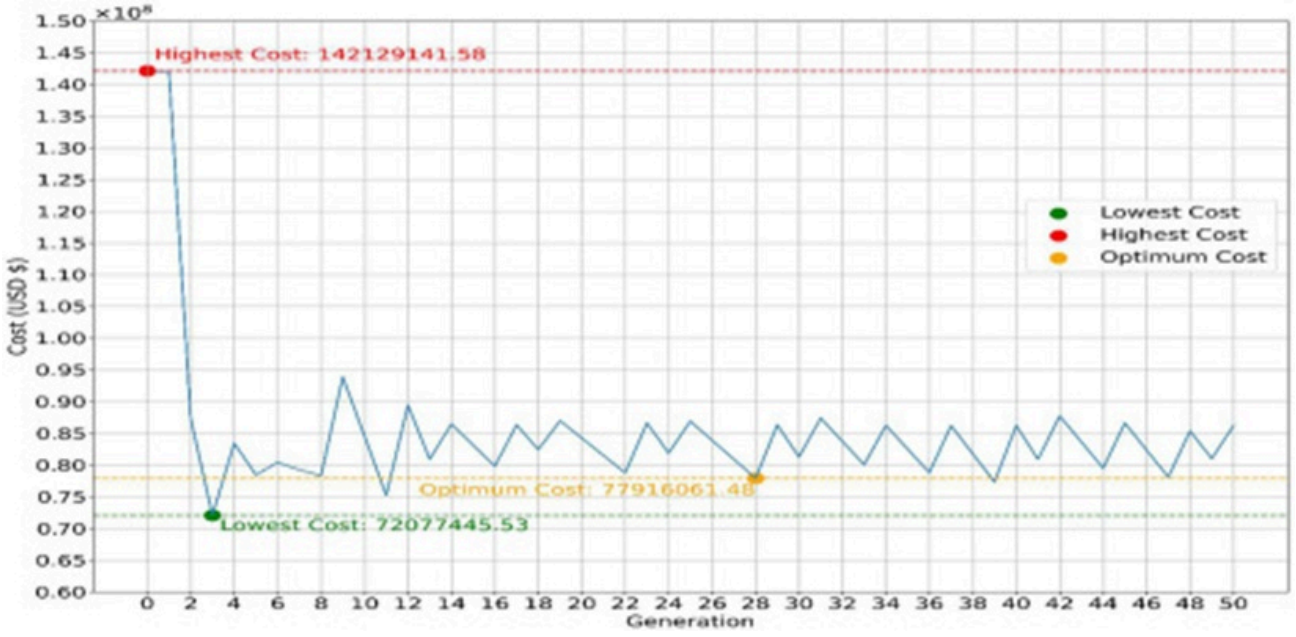

© 2023 The Author(s). | Published by Institute of Smart Energy Systems Press

Figure 10. Cost optimization (LCOE) across generations.

Figure 11 traces the path taken by GHG emissions, measured in metric tons, across the consecutive generations of the GMOT algorithm. In the early going, GHG emissions soar to a maximum near 3.29 billion tons. As the optimization advances, emissions are successfully compressed, with the routine zeroing in on an optimal figure of around 3.08 billion tons once the 28th generation is attained. This downward shift corresponds to a drop of close to 9% against actual emission volumes. The persistent erosion of GHG emissions generation after generation offers proof of the algorithm's capability to zero in on ecologically gentler energy compositions. Reaching such a reduction is no small matter for the fulfilment of EU climate commitments. It highlights the merit of embedding optimization tools like GMOT at the core of energy policy development.

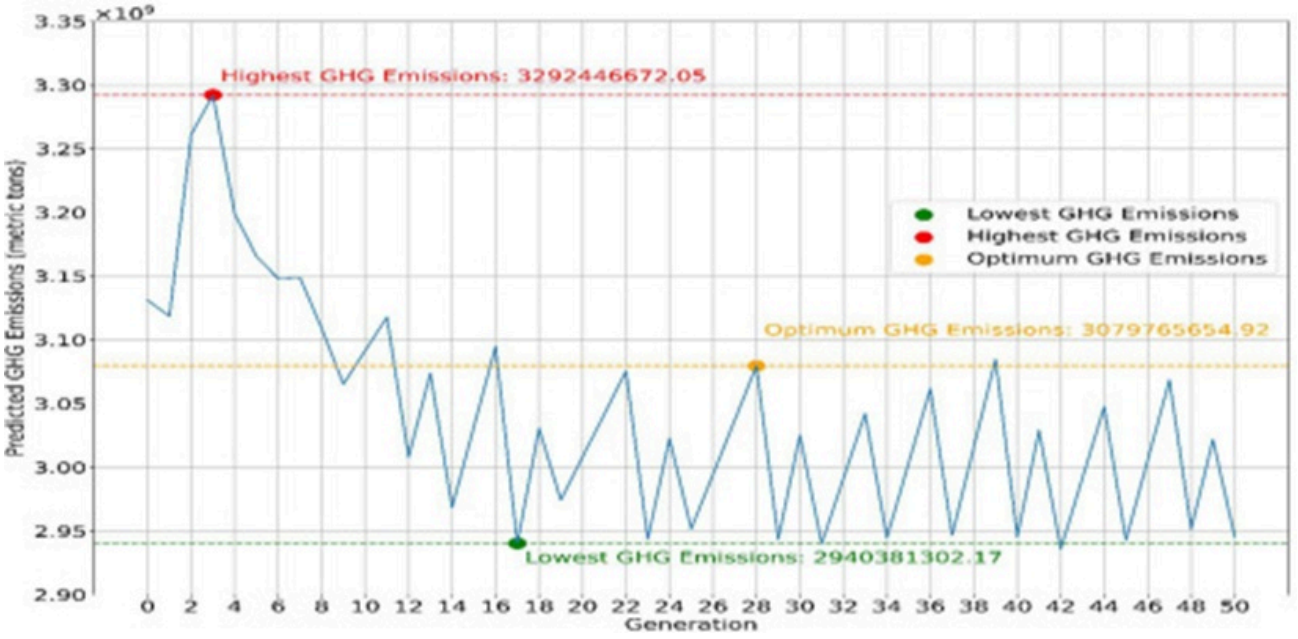

Figure 11. Greenhouse gas (GHG) emissions optimization across generations.

The optimization sequence indicated a pronounced reshuffling of the EU energy portfolio in the quest for the best possible results. Throughout the testing stage, a bolstered contribution from geo biomass, biofuels, solar, gas, and hydro energies came to the fore, all of which are conducive to GHG abatement. Running counter to this, GMOT advised a paring back of both coal and oil. This observation sits comfortably alongside other scholarly work in the area, where optimization models likewise found renewable sources to be championed—as exemplified in Kabeyi and Olanrewaju [56], which stresses how critical a move toward renewable and low-carbon grid electricity generation is for realizing sustainable energy ambitions.

Even though it remains classified as a fossil fuel, an expansion in the role of natural gas was proposed, presumably stemming from its comparatively lighter GHG footprint when juxtaposed with coal and oil [57]. Furthermore, GMOT advanced considerable gains on the economic front. In absolute terms, a steep descent of close to 46% in LCOE was secured, a development that could reverberate widely through the affordability landscape and the competitive dynamics among energy sources. This finding parallels other investigations that similarly concluded that energy optimization holds the potential to unlock substantial cost efficiencies [58].

As for GHG emissions, the optimization exercise exposed a sizeable scope for cutbacks, advancing a contraction of roughly 9% alongside current emission standings. Such a curtailment could assume a decisive part in the EU's broader push to counteract climate change. The subtle upward tick in energy imports that our model projects finds an echo in other studies that have observed a plausible role for energy imports inside optimized energy setups, particularly where

© 2023 The Author(s). | Published by Institute of Smart Energy Systems Press

the incoming energy is drawn from sustainable, low-emitting suppliers [56]. This observation highlights the potential importance of international cooperative frameworks for meeting energy optimization targets.

Technical analysis

Within **Figure 12**, the point judged to be optimal is pinpointed via the GMOT methodology advanced here, delivering a graphic illustration of the path taken by the optimization. During the initial generations, the scatter plot exhibits a diffuse spray of points. Inflated readings on every fitness axis typify these early-phase solutions, a telltale sign of their underwhelming showing with respect to cost, GHG emissions, and energy imports. As the optimization cycle pushes ahead into later generations, a clear tendency comes into view. The points incrementally coalesce into denser clusters, a signal that solution quality is climbing as they gravitate toward diminished values for the three fitness functions. This convergence dynamic makes it abundantly evident that, as generations accumulate, the optimization machinery churns out progressively better solutions, ultimately hitting the optimal point at generation 28 (Gen. 28).

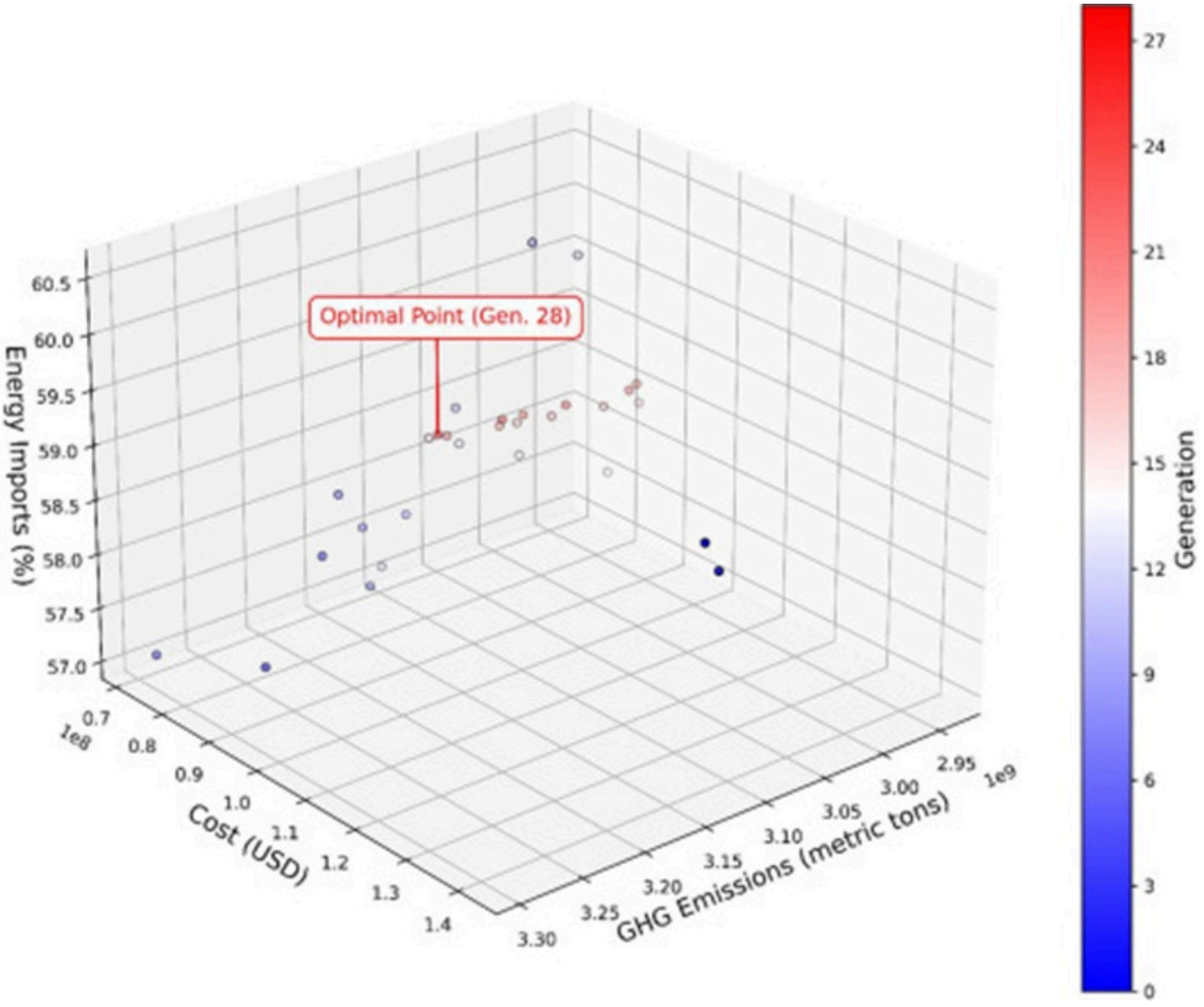

Figure 12. Visualization of neural network-enhanced gene modification technique convergence and optimal point across generations.

To demonstrate the strength of the GMOT method, benchmarking trials were conducted against two competing Pareto optimization distance formulations, using Euclidean distance and Normalized Euclidean distance as gauges within the

© 2023 The Author(s). | Published by Institute of Smart Energy Systems Press

objective space. These head-to-head assessments, set out in **Figures 13 and 14**, seek to deliver a quantitative window into the optimization voyage, its ultimate fruits, and the compromises it entails.

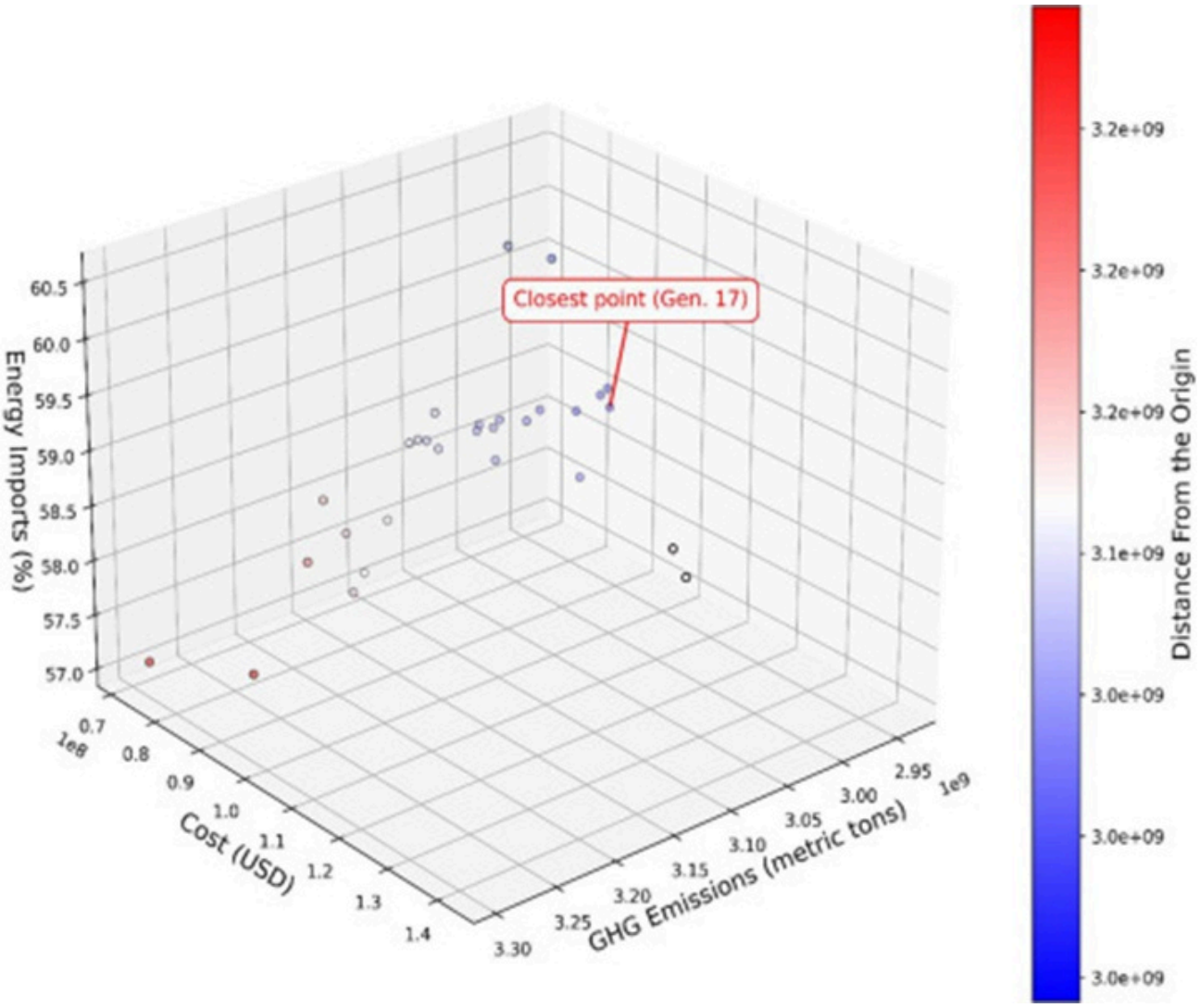

Figure 13. Visualization of Euclidean distance technique convergence and optimal point across generations.

© 2023 The Author(s). | Published by Institute of Smart Energy Systems Press

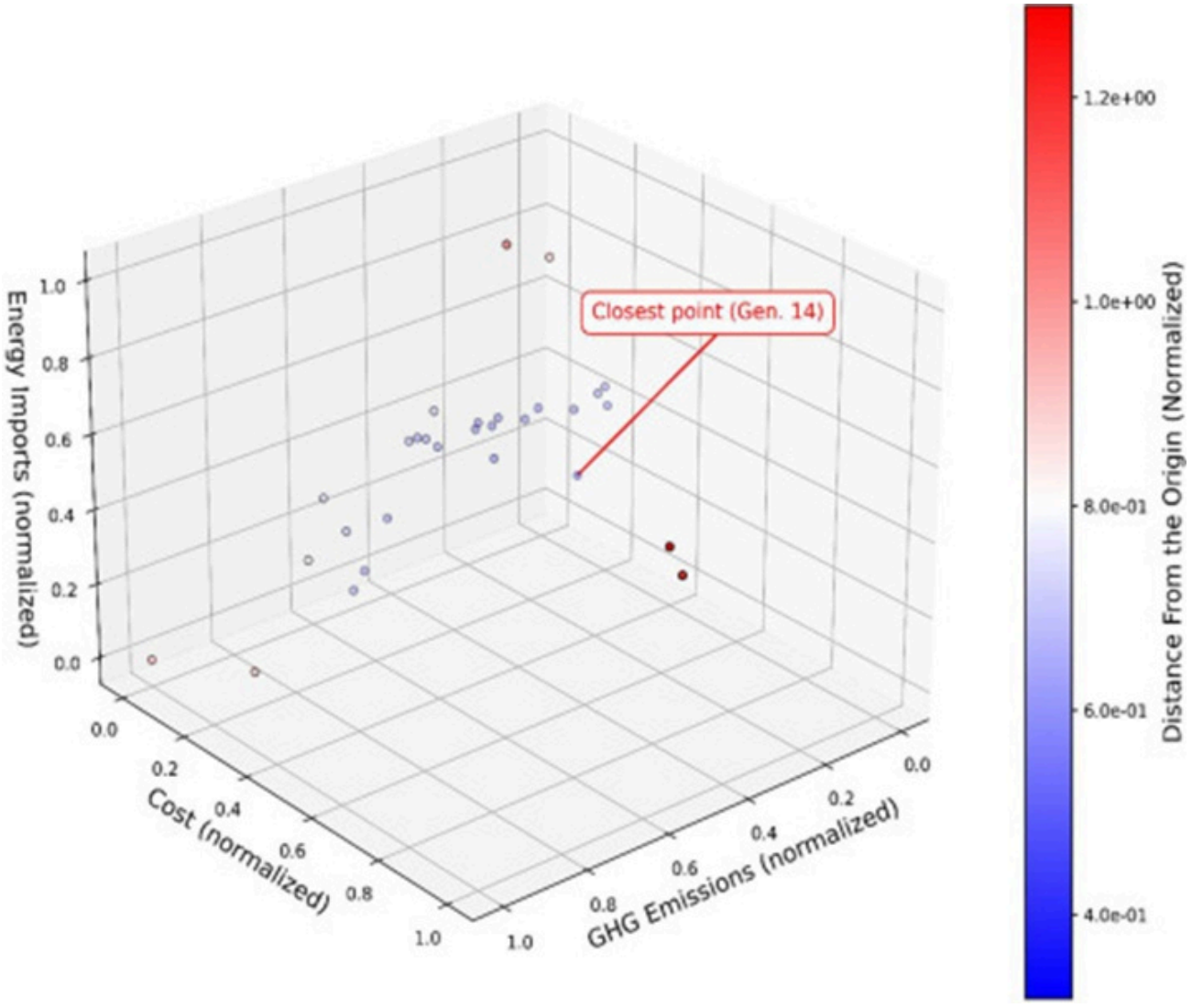

Figure 14. Visualization of normalized Euclidean distance technique convergence and optimal point across generations.

In **Figure 13**, Euclidean distance was used as the benchmark for assessing the optimization trajectory. Along this path, the optimization run isolated an optimal solution at generation 17 (Gen. 17), represented as the point closest to the origin. One must bear in mind, however, that Euclidean distance, by its very nature, does not automatically factor in mismatches in the scales spanning different objectives. As a consequence, it may favor solutions that excel along one particular objective dimension while possibly giving insufficient weight to the necessary concessions involving other objectives. This property of Euclidean distance is directly pertinent to our line of argument, given that it carries the risk of overinflating the weight carried by certain objectives—GHG emissions being a prime candidate—inside a multi-objective framework. This interplay is plainly visible in **Figure 13**, where points associated with greater GHG emission volumes (the objective that possesses the largest scale among the fitness functions) are found at a greater remove from the origin. Consequently, those points represent solutions that this distance-centric method rates as less attractive within the optimization sequence.

In **Figure 14**, the normalized Euclidean distance was used as the measuring rod for judging the optimization run. This approach yielded an optimal solution at generation 14 (Gen. 14), represented by the point closest to the origin. The preference for normalized Euclidean distance was prompted by the need to address unequal scales across the objectives, thereby striving to secure a more even-handed contribution from every objective across the optimization cycle.

© 2023 The Author(s). | Published by Institute of Smart Energy Systems Press

That being said, an Achilles' heel associated with normalized Euclidean distance cannot be overlooked. It may prove unequal to the task of neutralizing the pull exercised by objectives whose scales tower over the rest. This insight takes concrete form in **Figure 14**, where the points clustered in closest proximity to the origin are, by and large, those corresponding to lower GHG emissions (once more, the fitness function whose scale is the largest).

Figure 15 furnishes a comparative overview of the percentage alteration undergone by each fitness function, evaluated against the EU baseline for the calendar year 2021. This side-by-side examination weighs, in particular, the optimal outcomes harvested by GMOT at generation 28 against those logged by the Euclidean Distance method at generation 17 and the Normalized Euclidean Distance method at generation 14. The picture that emerges from the data is that GMOT distinguishes itself when the task involves refining fitness functions that are influenced by large-scale variables. The ascendancy of GMOT is unmistakable when it is compared alongside alternative strategies such as Euclidean Distance and Normalized Euclidean Distance. GMOT yields a formidable 46% reduction in costs, outstripping these rival approaches, each of which accomplishes a 40% cost reduction. This cost compression achieved by GMOT carries not only economic weight but also validates the method's detached, impartial posture toward optimization. In addition, GMOT chalked up a 9% fall in GHG emissions, a feat that is far from negligible given the convoluted character of large-scale variables. This underlines the resilience of GMOT when wrestling with thorny problems entailing several fitness functions, doing so in a fashion that is free of the slant that subjectivity can introduce into the optimization loop.

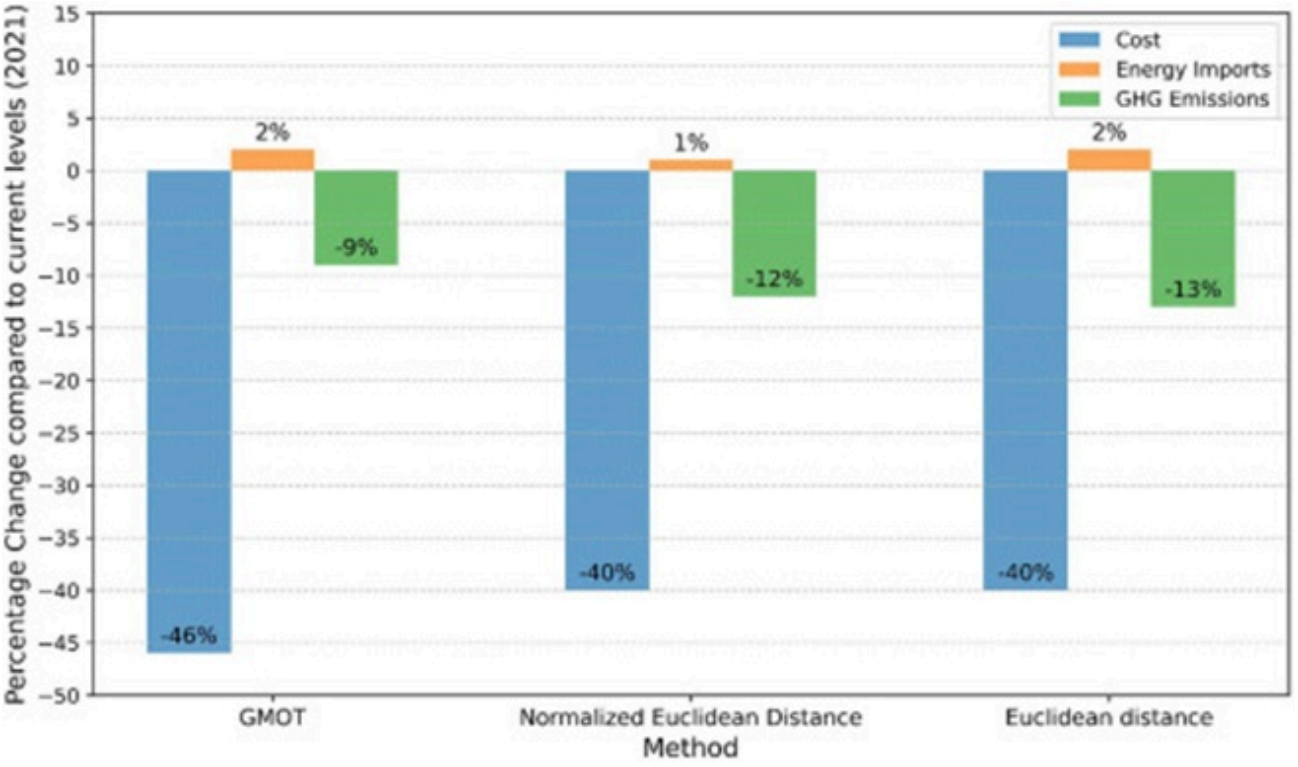

Figure 15. Performance comparison of optimization methods on cost, imports, and GHG emissions in the EU (2021 Baseline).

It warrants emphasis at this point that, while Euclidean Distance and Normalized Euclidean Distance notch up somewhat more favourable GHG emission curtailments—registering 13% and 12%, respectively—they log these figures in a manner that may come at the price of slighting other crucial facets, cost prominent among them. The genesis of this partiality rests first and foremost in the outsized magnitude of GHG emissions when held up against the other two variables. And yet, it is exactly this ingrained reflex to subjectively privilege GHG reduction ahead of cost considerations that illuminates how indispensable it is to field objective methods of the kind represented by GMOT. The faculty of GMOT to uphold an even-tempered and disinterested approach to optimization—grappling simultaneously with GHG emissions, cost, and

© 2023 The Author(s). | Published by Institute of Smart Energy Systems Press

energy import reduction without allowing any one dimension to dominate—marks it out as an instrument of exceptional value for tackling multi-faceted challenges that extend across a diverse spectrum of industrial sectors.

The Gene Modification Optimization Technique constitutes a consequential step forward in the realm of energy management optimization, leaving behind the capacities of standard algorithms such as ANFIS, grid search, and a range of multi-objective optimization frameworks—genetic algorithms, particle swarm optimization, and simulated annealing included. Instead of positioning itself as a direct rival to these long-standing methodologies, GMOT heralds a new conceptual model that taps into the prognostic muscle of ANNs to plot a course through the labyrinthine terrain of energy system optimization.

What most conspicuously differentiates GMOT is the way it leans on ANNs to anticipate the manifold knock-on effects that distinct assortments of energy sources produce for key metrics like cost, GHG emissions, and energy imports, all the while keeping within the guardrails defined by system constraints. This manner of operating represents a clean break from classical optimization practice, which habitually works off raw datasets or fixed, predefined fitness functions. Long-standing techniques commonly run aground when they come up against the elevated dimensionality and the dense web of mutual dependencies that are hallmarks of energy systems. They may base their optimization on coarse-grained models or linear data relationships, a practice that risks culminating in second-rate answers when thrust into the complex, non-linear interplay that defines real-world energy settings. GMOT, in stark contrast, enlists ANNs as nuanced predictive engines equipped to latch onto and mirror these entangled relationships with superior accuracy. The weaving of ANNs into the structural fabric of GMOT paves the way for a richer, more thorough combing of the solution space. Whereas traditional optimization routines might restrict their attention to a tight collection of pre-ordained variables or pared-down fitness functions, the ANN-anchored philosophy underpinning GMOT can entertain an immensely wider suite of possibilities. The reason lies in ANNs' aptitude to assimilate and reproduce the high-dimensional, convoluted connections that bind energy source configurations to their cascading impacts on cost, emissions, and imports.

This higher-level strategy equips GMOT to confront the staggering complexity of calibrating energy sources according to their actual configurations—a task that frequently exceeds the practical grasp of orthodox approaches, owing to the overwhelming profusion of variables and their tightly braided interdependencies.

By capitalizing on the predictive power of ANNs, GMOT can nimbly traverse this high-dimensional optimization terrain, offering solutions that stand out for their enhanced robustness and a more refined sensitivity to the subtleties of actual energy systems. GMOT does not simply line up alongside the roster of existing optimization instruments; it introduces a higher-order scaffold that is singularly attuned to the imperatives thrown up by present-day energy system optimization. Its proven capacity to channel the predictive vigour of ANNs toward the evaluation of complex fitness topographies cements GMOT's standing as a vanguard tool for contending with the layered difficulties that pervade energy management and optimization.

Conclusion

The study at hand presents the Neural Network-Enhanced Gene Modification Optimization Technique, engineered for multi-objective energy resource management. It demonstrates notable progress in fine-tuning energy consumption structures. This trailblazing framework fuses artificial intelligence with energy management by using neural network models as fitness functions, thereby projecting the effects of varied energy permutations on greenhouse gas emissions, energy outlays, and imports. A cardinal strength of this approach lies in its self-acting parameter configuration. This design feature substantially prunes back the encroachment of human partiality and reinforces the objectivity of the output. During simulation experiments anchored in European Union data, the technique generated striking dividends over the span of 28 optimization generations: a 46% shrinkage in the levelized cost of energy paired with a 9% rollback in greenhouse gas emissions, all the while preserving a steady equilibrium in energy imports. These results give ample testimony to the method's competence in threading a path through tangled, multi-dimensional optimization conundrums. To buttress its efficacy claims, the technique was held up against time-honoured methods such as Euclidean Distance, a

© 2023 The Author(s). | Published by Institute of Smart Energy Systems Press

comparison that bore out both its superior performance and its transparency. Beyond that, the built-in capacity to depict chromosomes and gene values in visual terms added a dimension of intelligibility to the optimization process, smoothing the path for interpreting and operationalizing the results. The technique's reliance on neural network forecasting models to map out the consequences of divergent energy configurations stands as a foundational innovation. This tactic squarely confronts the volatility tied to greenhouse gas emissions, costs, and imports, ensuring that the optimization process is built on accurate, data-driven forecasts. As a direct result, it measurably upgrades the precision of decision-making within energy management. By reducing the need for human involvement through automated parameter settings, the method not only removes sources of bias but also strengthens the trustworthiness of the optimization findings. Viewed in its entirety, this all-embracing approach marks a meaningful stride forward in the custodianship of energy resources, carrying with it the promise of uses that reach well past the confines of the energy domain and setting the stage for energy systems that marry heightened efficiency with deeper sustainability.

Acknowledgements

None

Conflict of interest

None

Financial support

Open Access funding provided by Hungarian Electronic Information Services National Programme (EISZ) - Corvinus University of Budapest.

Ethics statement

None

Received: 15 Aug 2022 Revised: 21 Oct 2022 Accepted: 07 Nov 2022
Published online: 15 November 2023

Rights and permissions

Open Access The author(s) retain copyright. This article is licensed under the Creative Commons Attribution-NonCommercial-ShareAlike 4.0 International License. It may be shared and adapted for non-commercial purposes with appropriate attribution, an indication of changes, and distribution of adaptations under the same license. Third-party material may be subject to separate terms identified in its credit line. View the license at https://creativecommons.org/licenses/by-nc-sa/4.0/.

References

1. IPCC. Summary for policymakers. In: Global Warming of 1.5°C. An IPCC Special Report on the Impacts of Global Warming of 1.5°C Above Pre-Industrial Levels and Related Global Greenhouse Gas Emission Pathways, in the Context of Strengthening the Global Response to the Threat of Climate Change, Sustainable Development, and Efforts to Eradicate Poverty. Geneva, Switzerland: World Meteorological Organization; 2018:32.

2. Bhowmik C, Bhowmik S, Ray A. Optimal green energy source selection: an eclectic decision. Energy Environ. 2020;31(5):842-59.

3. AlShafeey M, Csaki C. Tech mining analysis: renewable energy forecasting using artificial intelligence technologies. In: IEEE Nigeria 4th International Conference on Disruptive Technologies for Sustainable Development (NIGERCON); 2022:1-5.

4. Esily RR, Chi Y, Ibrahiem DM, Chen Y. Hydrogen strategy in decarbonization era: egypt as a case study. Int J Hydrogen Energy. 2022;47(42):18629-47.

5. Welsby D, Price J, Pye S, Ekins P. Unextractable fossil fuels in a 1.5 °C world. Nature. 2021;597(7875):230-4.

6. Bazilian M, Bradshaw M, Goldthau A, Westphal K. Model and manage the changing geopolitics of energy. Nature. 2019;569(7754):29-31.

7. Parsons J, Buongiorno J, Corradini M, Petti D. A fresh look at nuclear energy. Science. 2019;363(6423):105.

8. Buongiorno J, Parsons JE, Petti DA. The Future of Nuclear Energy in a Carbon-Constrained World. 2019.

9. Gernaat DE, de Boer HS, Daioglou V, Yalew SG, Müller C, van Vuuren DP. Climate change impacts on renewable energy supply. Nat Clim Chang. 2021;11(2):119-25.

10. Guerra OJ. Beyond short-duration energy storage. Nat Energy. 2021;6(5):460-1.

11. Bjørnskov J, Mortensen LK, Filonenko K, Shaker HR, Jradi M, Veje C. Optimization of district heating production with thermal storage using mixed-integer nonlinear programming with a new initialization approach. Energy Inform. 2021;4(1):1-17.

12. Long W, Wu T, Liang X, Xu S. Solving high-dimensional global optimization problems using an improved sine cosine algorithm. Expert Syst Appl. 2019;123:108-26.

13. Manna S, Loeffler TD, Batra R, Banik S, Chan H, Varughese B, et al. Learning in continuous action space for developing high dimensional potential energy models. Nat Commun. 2022;13(1):368.

14. Bre F, Fachinotti VD. A computational multi-objective optimization method to improve energy efficiency and thermal comfort in dwellings. Energy Build. 2017;154:283-94.

15. Cui Y, Geng Z, Zhu Q, Han Y. Multi-objective optimization methods and application in energy saving. Energy. 2017;125:681-704.

16. Von Homeyer I, Oberthür S, Jordan AJ. EU climate and energy governance in times of crisis: towards a new agenda. J Eur Public Policy. 2021;28(7):959-79.

17. Kuzemko C, Hadfield A. Defining and projecting EU energy policy. In: EU Leadership in Energy and Environmental Governance: Global and Local Challenges and Responses. 2016:21-50.

18. Blanco H, Nijs W, Ruf J, Faaij A. Potential for hydrogen and Power-to-Liquid in a low-carbon EU energy system using cost optimization. Appl Energy. 2018;232:617-39.

19. Spielhofer R, Schwaab J, Grêt-Regamey A. How spatial policies can leverage energy transitions− finding Pareto-optimal solutions for wind turbine locations with evolutionary multi-objective optimization. Environ Sci Policy. 2023;142:220-32.

20. Bazgan C, Ruzika S, Thielen C, Vanderpooten D. The power of the weighted sum scalarization for approximating multiobjective optimization problems. Theory Comput Syst. 2022;66(4):795-815.

21. Del Ser J, Osaba E, Molina D, Yang XS, Salcedo-Sanz S, Camacho D, et al. Bio-inspired computation: where we stand and what's next. Swarm Evol Comput. 2019;48:220-50.

© 2023 The Author(s). | Published by Institute of Smart Energy Systems Press

22. Merk T, Peterson V, Köhler R, Haufe S, Richardson RM, Neumann WJ. Machine learning based brain signal decoding for intelligent adaptive deep brain stimulation. Exp Neurol. 2022;351:113993.

23. Roald LA, Pozo D, Papavasiliou A, Molzahn DK, Kazempour J, Conejo A. Power systems optimization under uncertainty: a review of methods and applications. Electr Power Syst Res. 2023;214:108725.

24. Gunantara N. A review of multi-objective optimization: methods and its applications. Cogent Eng. 2018;5(1):1502242.

25. Kasem MM. Multiobjective design optimization of parabolic trough collectors. Sci Rep. 2022;12(1):19964.

26. Antunes CH. Multiobjective optimization in the energy sector: selected problems and challenges. In: New Perspectives in Multiple Criteria Decision Making: Innovative Applications and Case Studies. 2019:357-70.

27. Miettinen K. Nonlinear Multiobjective Optimization. Springer Science & Business Media; 1999.

28. Kim IY, De Weck OL. Adaptive weighted-sum method for bi-objective optimization: pareto front generation. Struct Multidiscip Optim. 2005;29(2):149-58.

29. Odu G, Charles-Owaba O. Review of multi-criteria optimization methods–theory and applications. IOSR J Eng. 2013;3(10):01-14.

30. Saini N, Saha S. Multi-objective optimization techniques: a survey of the state-of-the-art and applications: multi-objective optimization techniques. Eur Phys J Spec Top. 2021;230(10):2319-35.

31. Krzywanski J, Skrobek D, Zylka A, Grabowska K, Kulakowska A, Sosnowski M, et al. Heat and mass transfer prediction in fluidized beds of cooling and desalination systems by AI approach. Appl Therm Eng. 2023;225:120200.

32. Ashraf WM, Uddin GM, Arafat SM, Krzywanski J, Xiaonan W. Strategic-level performance enhancement of a 660 MWe supercritical power plant and emissions reduction by AI approach. Energy Convers Manag. 2021;250:114913.

33. Krzywanski J, Grabowska K, Sosnowski M, Żyłka A, Sztekler K, Kalawa W, et al. Modeling of a re-heat two-stage adsorption chiller by AI approach. MATEC Web Conf. 2018;240:05014.

34. Li Y, Yan Z. Improved shuffled frog leaping algorithm on system reliability analysis. Brain Inform. 2019;6(1):1-7.

35. Chen B, Liu Q, Chen H, Wang L, Deng T, Zhang L, et al. Multiobjective optimization of building energy consumption based on BIM-DB and LSSVM-NSGA-II. J Clean Prod. 2021;294:126153.

36. Jiang M, An H, Gao X, Liu D, Jia N, Xi X. Consumption-based multi-objective optimization model for minimizing energy consumption: a case study of China. Energy. 2020;208:118384.

37. Shboul B, Zayed ME, Tariq R, Ashraf WM, Odat AS, Rehman S, et al. New hybrid photovoltaic-fuel cell system for green hydrogen and power production: performance optimization assisted with Gaussian process regression method. Int J Hydrogen Energy. 2024;59:1214-29.

38. Bischl B, Binder M, Lang M, Pielok T, Richter J, Coors S, et al. Hyperparameter optimization: foundations, algorithms, best practices and open challenges. arXiv. 2021. arXiv:2107.05847.

39. Arnold C, Biedebach L, Küpfer A, Neunhoeffer M. The role of hyperparameters in machine learning models and how to tune them. Political Sci Res Methods. 2023:1-8.

40. Joo H, Bao C, Sen I, Huang F, Battle L. Guided hyperparameter tuning through visualization and inference. arXiv. 2021. arXiv:2105.11516.

© 2023 The Author(s). | Published by Institute of Smart Energy Systems Press

41. Deb K. Multi-Objective Optimization Using Evolutionary Algorithms. John Wiley & Sons; 2001.

42. Treanţă S, Jha S, Khan MB, Saeed T. On some constrained optimization problems. Mathematics. 2022;10(5):818.

43. Adihou Y, Mabrouk MT, Haurant P, Lacarrièere B. A multi-objective optimization model for the operation of decentralized multi-energy systems. J Phys: Conf Ser. 2019;1343:012104.

44. Eichfelder G, Quintana E, Rocktäschel S. A vectorization scheme for nonconvex set optimization problems. SIAM J Optim. 2022;32(2):1184-209.

45. Rudin C, Chen C, Chen Z, Huang H, Semenova L, Zhong C. Interpretable machine learning: fundamental principles and 10 grand challenges. Stat Surv. 2022;16:1-85.

46. IEA. Outlook for Biogas and Biomethane: Prospects for Organic Growth. Paris, France: IEA; 2020:1-93.

47. Brown C, Foley B. Achieving a Cost-Competitive Offshore Wind Power Industry: What is the Most Effective Policy Framework? 2015.

48. AlShafeey M, Rashdan O. Quantifying the impact of energy consumption sources on GHG emissions in major economies: a machine learning approach. Energy Strategy Rev. 2023;49:101159.

49. Hagan MT, Menhaj MB. Training feedforward networks with the Marquardt algorithm. IEEE Trans Neural Netw. 1994;5(6):989-93.

50. Artacho FA, Dontchev AL, Gaydu M, Geoffroy MH, Veliov VM. Metric regularity of Newton's iteration. SIAM J Control Optim. 2011;49(2):339-62.

51. Damadi S, Moharrer G, Cham M, Shen J. The backpropagation algorithm for a math student. In: 2023 International Joint Conference on Neural Networks (IJCNN); 2023:01-09.

52. Tian Y, Zhu W, Zhang X, Jin Y. A practical tutorial on solving optimization problems via PlatEMO. Neurocomputing. 2023;518:190-205.

53. Van Ruijven BJ, De Cian E, Sue Wing I. Amplification of future energy demand growth due to climate change. Nat Commun. 2019;10(1):2762.

54. Sayed M, Gharghory SM, Kamal HA. Euclidean distance-based multi-objective particle swarm optimization for optimal power plant set points. Energy Syst. 2016;7(4):569-83.

55. He L, Ishibuchi H, Trivedi A, Wang H, Nan Y, Srinivasan D. A survey of normalization methods in multiobjective evolutionary algorithms. IEEE Trans Evol Comput. 2021;25(6):1028-48.

56. Kabeyi MJB, Olanrewaju OA. Sustainable energy transition for renewable and low carbon grid electricity generation and supply. Front Energy Res. 2022;9:1032.

57. Wang Q, Guo J, Li R, Jiang X. Exploring the role of nuclear energy in the energy transition: a comparative perspective of the effects of coal, oil, natural gas, renewable energy, and nuclear power on economic growth and carbon emissions. Environ Res. 2023;221:115290.

58. Carvalho MM, Fleury A, Lopes AP. An overview of the literature on technology roadmapping (TRM): contributions and trends. Technol Forecast Soc Change. 2013;80(7):1418-37.

© 2023 The Author(s). | Published by Institute of Smart Energy Systems Press